**I. M. Pazukha, I. Yu. Protsenko**

# THEORETICAL METHODS
# OF INVESTIGATION OF THIN FILM
# MATERIALS PROPERTIES

Study guide

Recommended by the Academic Council of Sumy State University

УДК 621.793+538.975](075.8)
   Р35

*Recommended for publication*
*by the Scientific Council of Sumy State University*
*as a study guide*
*(minutes № 8 of 09.02.2017)*

**Pazukha I. M.**

Р35     Theoretical methods of investigation of thin film materials properties : study guide / I. M. Pazukha, I. Yu. Protsenko. – Sumy : Sumy State University, 2017. – 102 p.
   ISBN 978-966-657-682-1

The study guide contains theoretical methods of thin metallic films materials properties investigation, particularly theoretical methods for size effects in electrical resistivity and strain of thin films and double-layer thin film systems. The interpretation of experimental data in the term of different theoretical methods is presented.

The study guide is intended for students of institution of higher education in the field "Electronics" and qualification level "Master".

**УДК 621.793+538.975](075.8)**

# CONTENTS

# INTRODUCTION

The wide application of thin film materials in different fields of electronics (micro-, nanoelectronics et al.) stimulates carrying out and further development of experimental and theoretical methods of investigation of their physical properties. It is well known that thin film materials are characterized by physical properties, which significantly differ from similar in bulk state. It is associated with two mean reasons. The first one is dependence of thin film crystal structure from preparation conditions. The second one is physical properties dependence from thickness or other thin film linear size. Since experimental and theoretical methods supply each other, after studying the first one in the frame of bachelor level the logical continuation is studying theoretical methods that require more substantial mathematical prerequisite. For this reason our English courses (at parallel studying in Ukrainian) are a part of education program of master level.

Since size effects (SE) in electrophysical properties play an important role in physical properties of thin film materials it will be the main subject of analysis in the frame of this study guide. In consideration that thermodynamic SE play less marked role we proposed to students another study guide which reviews all questions according to thermodynamics of small size systems.

The study guide contains problems, which are pointed at developing students' problem-solving ability.

The authors appreciate reviewers Professor Lopatkin Yu. M. and Ph. D. Danylchenko S. M. for their comments relative to study guide content.

# SECTION 1
## Size effects in electrical resistivity of thin films

### 1.1 Introduction

Thin film materials are widely used at developing microelectronics resource base, different types of sensors and devices because of their unique physical properties in comparison with materials in bulk state. There are two types of effects in films which can change their physical properties. One type is related to film structural state (amorphous, mono- or polycrystalline) and the other one to size effect phenomenon. Size effect is dependence of physical properties on film thickness or mean grain size. Investigations of these effects are important for better understanding thin film physical properties and their usefulness in practical application.

The size effect (SE) in electrophysical properties appears when mean free path of charge carrier ($\lambda$) is comparable to the film thickness ($d$). In this section, the SE in electrical resistivity of thin film materials is considered from the point of view that mean free path of charge carrier is bordered by internal surface of the films or geometrical size of crystallites. In the first case, parameters, such as, resistance ($R$) or temperature coefficient of resistance (TCR), depend on thin film thickness, and external size effect (ESE) appears. In the second case, parameters depend on mean size of crystallites and internal size effect (ISE) appears.

### 1.2 The geometry of thin film and types of electron scattering

The geometry of thin films with thickness $d$ considered in this section is shown in Fig. 1.1. It is assumed that film has isotropic bulk mean free paths $\lambda_0$ and fine-grain crystallites with an average size $L$.

6
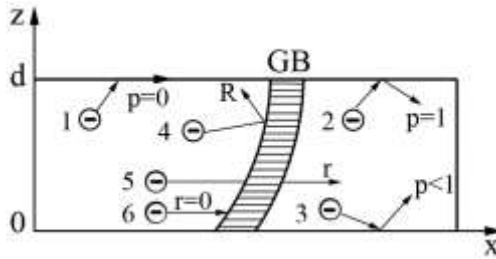
Figure 1.1 – The geometry of thin film and types of electron scattering: $p$ is the specularity parameter; $R$ is the reflection parameter; $r$ is the transmission parameter; GB is grain boundary

The resistivity ($\rho$) is a base parameter which affects electronic, strain, magnetic, etc. properties of thin film materials. The value of resistivity increases when the film thickness and mean free path became of the same order. In general case there is a great number of types of electron scattering which changed total value of resistivity. However, at theoretical interpretation of size effect the following various idealized sources of scattering are considered:

1. External surfaces of the film.

This source of scattering is described by the specularity parameter $p$. Specularity parameter $p$ is a probability of electron scattering on the external surfaces of the films. In the case when $p = 0$ the electron scattering at external surfaces is diffusive and scattered electrons slide along surfaces and do not contribute to the electrical resistance.

2. Grain boundary.

Grain boundaries can be represented as array of scattering planes. This source of scattering is described by electronic reflection coefficient $R$, which defines the probability of electron reflection at the grain boundaries and

transmission coefficient *r* which defines the probability of coherent passage of the electron across the grain boundaries.

### 1.3 The Fuchs and Sondheimer (FS) model for metal films

The first time systematical investigation of the thicknesses influence on the film resistance was done by Fuchs (1938) and Sondheimer (1950–1952) (the Fuchs and Sondheimer model).

The FS model can be summarized as follows:
– model described size dependence of resistivity for monocrystalline thin film;
– film has isotropic bulk mean free paths $\lambda_0$;
– the electron scattering on grain boundaries is not taken into account;
– scattering at the external film surfaces is described by specularity parameter *p*. The value of this parameter is limited by the condition $0 \leq p < 1$, $p = 0$ is the case of entirely diffuse scattering, $p = 1$ is the case of entirely specular scattering;
– the simplest boundary condition is obtained by assuming that the electron scattering at external surfaces is entirely diffuse ($p = 0$) so that the electrons do not contribute to the electrical current.

The geometry of the FS model is presented in Fig. 1.2. Thin film limited by the surfaces $z = 0$ and $z = d$ is subjected to
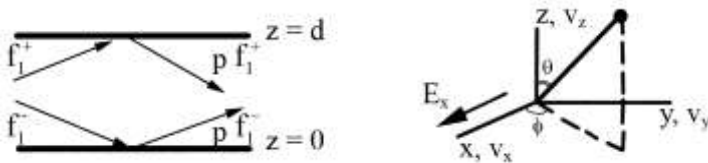


Figure 1.2 – The geometry of FS model [10]

8

an electrical field $E$ in the $x$ direction.

It is necessary to solve the kinetic equation of Boltzmann to obtain functional dependency $\rho(d)$:

$$-\frac{e}{m^*} \cdot \vec{E} \cdot grad_{\vec{\upsilon}} f + \vec{\upsilon} \cdot grad_{\vec{r}} f = \left( \frac{\partial f}{\partial t} \right), \qquad (1.1)$$

where $\left( \dfrac{\partial f}{\partial t} \right) = -\dfrac{f - f_o}{\tau}$ – collision integral which describes

collision of electrons with phonons or with imperfections in the lattice, $f_0$ is the equilibrium distribution (distribution function when the electrical field is absence), $f$ is a deviation from the Fermi-Dirac function $f_0$ induced by the electrical field $E$, $\tau = 10^{-9}$ seconds is the relaxation time (the time of electrons transition from $f$ to $f_0$ state), $e$ is the electron charge, $m^*$ is the electron effective mass, $\upsilon$ is the electron velocity.

The distribution function $f$ of the electrons for the film in the electrical field can be written as

$$f = f_0 + f_1(\upsilon, z), \qquad (1.2)$$

where $f_1(\upsilon, z)$ depends on the space variables only through $z$.
For electrical field $E_x$ applied in the $x$ direction, the equation is (1.1) reduced to

$$\frac{\partial f_1}{\partial z} + \frac{f_1}{t \cdot \upsilon_z} = \frac{eE}{m^* \upsilon_z} \cdot \frac{\partial f_0}{\partial \upsilon_z}. \qquad (1.1')$$

The calculation of the current density $J(z)$ across the thickness $d$ starts with the formula

$$J(z) = -2e \left( \frac{m^*}{h^3} \right) \iiint\limits_{x_x \, x_y \, x_y} \upsilon_x f_1 d\upsilon_x d\upsilon_y d\upsilon_z. \qquad (1.3)$$

To obtain overall equation for electrical conductivity the integration of (1.3) is carried out over $z$:

$$\sigma = \frac{1}{E_x d} \int_0^d J(z)\,dz. \tag{1.4}$$

Taking into account that $\rho = 1/\sigma$ we obtain the general equation of the FS model for resistivity

$$\frac{\rho}{\rho_\infty} = \left[ 1 - \frac{3\lambda_0(1-p)}{8d} \int_1^\infty (t^{-3} - t^{-5}) \frac{1-e^{kT}}{1-pe^{kT}} dt \right]^{-1}, \tag{1.5}$$

where $\rho_\infty$ is the resistivity of bulk material with the same type and concentration of defects as in the thin film, $\lambda_0$ is the mean free path of electrons in bulk material, $k$ is the reduced thickness i. e. the ration of the film thickness $d$ to the mean free path $\lambda_0$ ($k = \dfrac{d}{\lambda_0}$), $t = \cos^{-1}\Theta$, where $\Theta$ is angle between velocity vector $\upsilon$ and direction $z$.

The limiting form of equation (1.5) for thick films is

$$\frac{\rho}{\rho_\infty} = \frac{\rho_f}{\rho_0} = 1 + \frac{3}{8}\frac{\lambda_0(1-p)}{d}, \quad k \gg 1, \tag{1.7}$$

and for very thin films

$$\frac{\rho}{\rho_\infty} = \frac{\rho_f}{\rho_0} = \frac{4}{3}\frac{1-p}{1+p}\frac{\lambda_0}{d}\left( \ln\frac{\lambda_0}{d} \right)^{-1}, \quad k \ll 1, \tag{1.8}$$

where $\rho_0$ is the resistivity of bulk monocrystalline, $\rho_f$ is resistivity of the film.

Theoretical values for the resistivity ratio $\rho_f/\rho_0$ as a function of the reduced thickness $k$ are presented in Fig. 1.3.
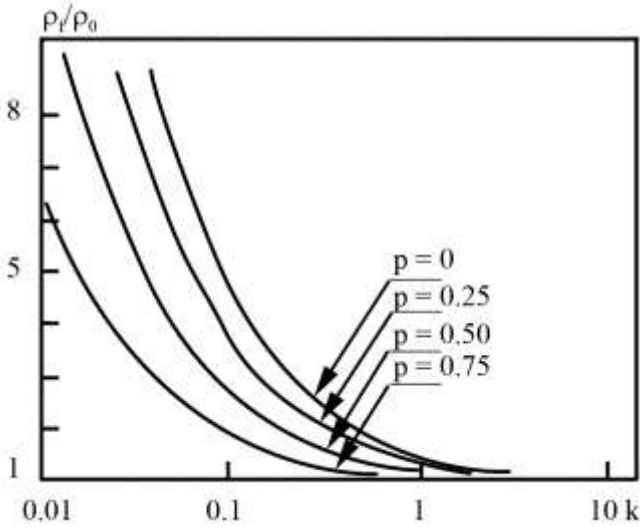


Figure 1.3 – Theoretical dependences of relative changes in the resistivity $\rho_f/\rho_0$ compared to reduced thickness $k$ for different values of specularity coefficient $p$

## 1.4 The method of experimental determination of FS parameters

The main equation of FS model is difficult for calculation and comparison with experimental data, so for interpreted experiments on thin film resistivity in terms of FS theory it is reasonable to fit data with limiting forms (1.7) and (1.8).

Generally, to compare experimental data with the calculation data on the base of the limiting forms of FS model it is necessary to linearize the equations (1.7) or (1.8).

### 1.4.1 The limiting case of FS model for thick films

Let's consider the case $k \gg 1$.
The equation (1.7) can be rewritten in the form:
a) $k \gg 1$, when $d \gg \lambda_0$ but $T$ is normal or when $T$ is low and $d$ is normal (see Fig. 1.4):

$$\rho = \rho_\infty + \frac{3}{8}\frac{\lambda_0(1-p)}{d}\rho_\infty \text{ or} \qquad (1.7')$$

b) $k \ll 1$, when $d \ll \lambda_0$ but $T$ is normal or when $T$ is high and $d$ is normal (see Fig. 1.4):

$$\rho d = \rho_\infty d + \frac{3}{8}\lambda_0(1-p)\rho_\infty. \qquad (1.7'')$$

The equation $(1.7'')$ is the equation of a straight line $\rho d = A + Bd$ with a slope of the resisitivity of bulk material $\rho_\infty$ and an ordinate intercept of $A = 3\lambda_0(1-p)\rho_\infty/8$ (Fig. 1.5).
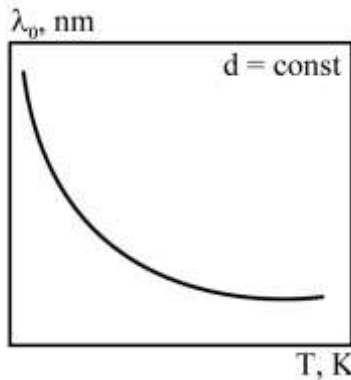


Figure 1.4 – Temperature dependence of mean free path for thin film materials at $d = $ const
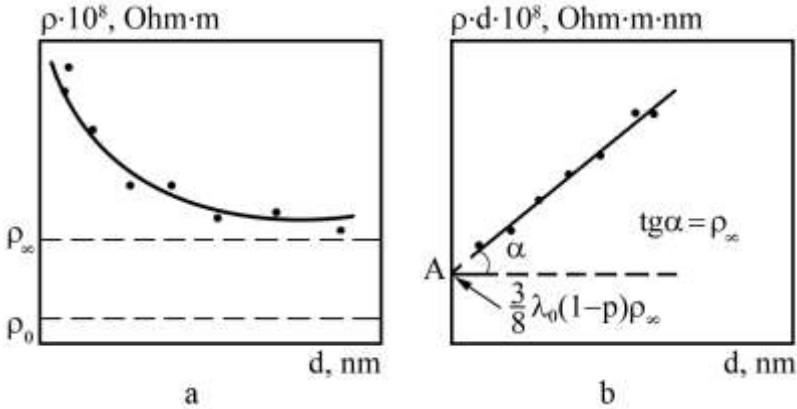
Figure 1.5 − Experimental size dependence of the thin film resistivity (a) and dependence $\rho d$ compared to $d$ (the limiting case of FS model for thick films) (b). The values of $\rho_\infty$ and $\rho_0$ are the asymptotes of exponential dependence

Obtaining a slope equal to the value of $\rho_\infty$, one cannot deduce separately the value of $\lambda_0$ and $(1-p)$ from the ordinate intercept. The estimation of mean free path value can be done in the case of entirely diffuse scattering ($p = 0$).

### 1.4.2 The limiting case of FS model for very thin films

According to above procedure it appears that a procedure for determining the electrical parameters in the case of very thin film consist of the next steps:

1) rewriting the equation (1.8) in the form

$$\rho = \frac{4}{3}\frac{1-p}{1+p}\frac{\lambda_0}{d}\left(\ln\frac{\lambda_0}{d}\right)^{-1}\rho_\infty \text{ or} \qquad (1.8')$$

$$(\rho d)^{-1} = \frac{3}{4}\frac{1+p}{1-p}\frac{1}{\lambda_0 \rho_\infty}(\ln \lambda_0 - \ln d); \qquad (1.8'')$$

2) plotting the data in the form $(\rho d)^{-1}$ compared to $\ln d$ to determine the value of mean free path (Fig. 1.6). The abscissa intercept is value of $\ln d = \ln \lambda_0$;
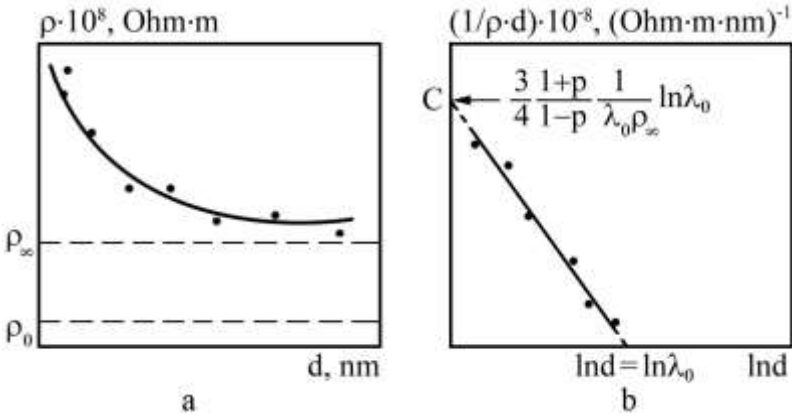


Figure 1.6 – Experimental size dependence of the thin film resistivity (a) and dependence $1/\rho d$ compared to $\ln d$ (the limiting case of the FS model for very thin films) (b)

3) using the value of specularity parameter $p = 0$ find the value of resistivity of bulk material $\rho_\infty$. The ordinate intercept is value of $C = \frac{3}{4}\frac{1+p}{1-p}\frac{1}{\lambda_0 \rho_\infty}\ln \lambda_0$.

Note, that the same experimental results coordinate with FS model, whereas others show marked departures that may be attributed to significant grain boundary scattering. Besides, experimental size dependence $\rho(d)$ is out of keeping to hyperbolic law $\rho \sim d^{-1}$ which follows from FS model.

## 1.5 Theoretical bases of Mayadas – Shatzkes (MS) model

The theoretical model for total film resistivity was proposed by Mayadas and Shatzkes. According to their framework the grain boundaries can be represented as parallel, partially reflecting planes, randomly spaced but perpendicular both to the field $E$ and to the plane of the film.

The distribution function $f_1(v,z)$ of the conduction electrons is assumed to be due to the superimposed effects of background scattering and of scattering at the grain boundaries. In this case the kinetic equation of Boltzmann for infinitely thick film can be written as

$$eE_x \upsilon_x \cdot \frac{\partial f_0(k)}{\partial \varepsilon} = \int p_1(k,k')[f_1(k) - f_1(k')]dk + \frac{1}{\tau_0}f_1(k)$$

(1.9)

with the same notation as in paragraph 1.3. The value $p_1(k, k')$ is transition probability for an electronic state $k$ to state $k'$ by grain boundaries.

The solution for Boltzmann's equation is

$$f_1(k) = \tau_1^* eE_x \upsilon_x \frac{\partial f_0}{\partial \varepsilon},$$

(1.10)

where the relaxation time $\tau_1^*$ is related to both the background and grain boundary scattering and can be obtained in the form

$$\frac{1}{\tau^*} = \frac{1}{\tau_0} + \frac{\alpha}{\tau_0}\frac{k_F}{|k_F|},$$

(1.11)

where $k_F$ is the magnitude of Fermi wave vector.

15

An approximation equation for current density $J_x$ is

$$J_x = \sigma_g E_x, \quad \frac{\pi BT}{\varepsilon_F} << 1, \tag{1.12}$$

where $B$ is Boltzmann's constant with

$$\sigma_g = \sigma_0 \cdot f(\alpha), \tag{1.13}$$

$$f(\alpha) = 1 - \frac{3}{2}\alpha + 3\alpha^2 - 3\alpha^3 \ln\left(1 + \frac{1}{\alpha}\right), \tag{1.14}$$

$$\alpha = \frac{\lambda_0}{L} \cdot \frac{R}{1-R}, \tag{1.15}$$

where $\sigma_g$ is the conductivity of infinitely thick polycrystalline film, $f(\alpha)$ is the function of grain boundary scattering, $\alpha$ is scattering parameter, $L$ is the mean grain size, $R$ is the specular reflection parameter at the grain boundaries.

The general expression of the film resistivity is derived from the resistivity equation obtained in the FS model and gives

$$\rho = \left\{ \frac{1}{\rho_g} - \frac{6(1-p)}{\pi k \rho_0} \int\limits_0^{\pi/2} d\Phi \int\limits_1^\infty dt \frac{\cos^2 \Phi}{H^2(t,\Phi)} \left( t^{-3} - t^{-5} \frac{1 - e^{-[ktH]}}{1 - p e^{-[ktH]}} \right) \right\}^{-1}, \tag{1.16}$$

where $\rho_g$ is the resistivity of infinitely thick polycrystalline film, $H(t,\Phi) = 1 + \dfrac{\alpha}{\cos\Phi\sqrt{1-t^2}}$, $t = \cos^{-1}\Theta$, where $\Theta$ is angle between velocity vector $\upsilon$ and direction $z$.

## 1.6 The approximation relationship of Tellier, Tosser and Pichard

### 1.6.1 The effective mean free path model

The theoretical model proposed by Mayadas and Shatzkes is very difficult for determination of electrical parameters. So Tellier, Tosser and Pichard proposed several alternative methods of MS model simplification.

Mayadas and Shatzkes have suggested that it might be hoped that an "effective intrinsic mean free path" can be definable for a polycrystal, but no theoretical basis has been proposed for sustaining this physical point of view.

The theoretical validity of this empirical assumption can be established by assuming that a unique mean free path can represent the electronic scattering from sources other than external surfaces. This unique mean free path is called "effective" mean free path $\lambda_g$ and is defined by

$$\lambda_g = \lambda_0 \cdot f(\alpha).$$  (1.17)

The Boltzmann equation then becomes

$$eE_x \upsilon_x \cdot \frac{\partial f_0}{\partial \varepsilon} = \frac{f_0(k)}{\tau_0 \cdot f(\alpha)} + \upsilon_x \frac{\partial f_1(k)}{\partial z}.$$  (1.18)

The main equation for the reduced resistivity is

$$\frac{\rho}{\rho_0} = \left[ 1 + \frac{3}{8} \frac{\lambda_0 (1-p)}{d} f(\alpha) \right] \cdot f(\alpha)^{-1}.$$  (1.19)

At $(f(\alpha) \to 1)$ the equation of "effective" mean free path model is similar to the main equation of FS model.

For temperature coefficient of resistance (TCR) the equation (1.19) can be rewritten as

$$\frac{\beta}{\beta_0} = \left[1 + \frac{3}{8}\frac{\lambda_0(1-p)}{d}f(\alpha)\right]^{-1} \cdot \left[1 + \frac{g(\alpha)}{f(\alpha)}\right], \qquad (1.20)$$

where $\beta_0$ is the temperature coefficient of resistance of bulk monocrystalline material, $g(\alpha) = \alpha \cdot \dfrac{df}{d\alpha}$.

Protsenko et al. shown that equation (1.20) for TCR can be simplified. Using the method of numerical calculation it has been shown that value of multiplier $1 + \dfrac{g(\alpha)}{f(\alpha)}$ is equal to value of grain boundary scattering function, i. e. $1 + \dfrac{g(\alpha)}{f(\alpha)} = f(\alpha)$ at $\alpha \le 10$.

In this case the equation (1.20) yields

$$\frac{\beta}{\beta_0} = \left[1 + \frac{3}{8}\frac{\lambda_0(1-p)}{d}f(\alpha)\right]^{-1} \cdot f(\alpha)\left[1 + \frac{g(\alpha)}{f(\alpha)}\right] \qquad (1.20')$$

and on the assumption that $\dfrac{3}{8}\dfrac{\lambda_0(1-p)}{d}f(\alpha) <<1$ the equation (1.20) then becomes

$$\frac{\beta}{\beta_0} = \left[1 - \frac{3}{8}\frac{\lambda_0(1-p)}{d}f(\alpha)\right] \cdot f(\alpha). \qquad (1.20'')$$

There are two methods of determination of values of $\lambda_0(1-p)$ and $R$. The first one is comparison of experimental and fit data with equations (1.19) and (1.20''). The correct result

corresponds to minimum deviation of experimental and calculated data. The second one is joint solution of equations (1.20) and (1.20´´) that allowed to obtain dependences of $\lambda_0(1 - p)$ from thickness $d$ or grain size $L$.
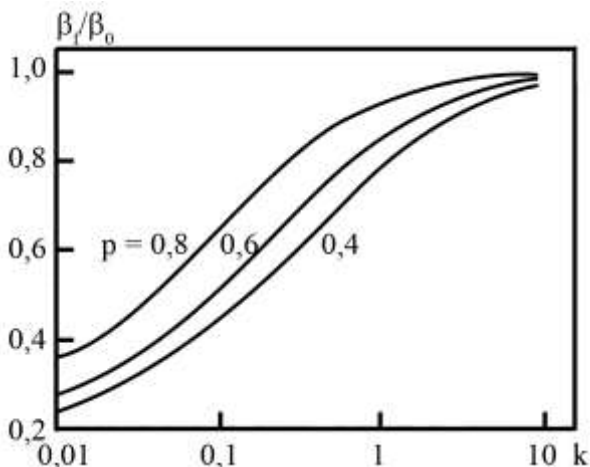


Figure 1.7 – Theoretical dependences of the reduced TCR $\beta/\beta_0$ plotted against the reduced thickness $k$ for different values of the specularity parameter $p$

Figure 1.7 shows the theoretical variations of the reduced TCR $\beta/\beta_0$ with the reduced thickness $k$ for different values of the specularity parameter. The curves exhibit several features:

1) the size effect vanishes for large reduced thicknesses;

2) for the given thickness the TCR increases, as expected, with increasing values of the specularity parameter $p$.

### 1.6.2 The linearized model

This method of simplification is linearization of general equation of the resisitivity in the MS model (1.16).

In the case of polycrystalline thick films the equations for the resisitivity takes form:

$$\rho_f/\rho_0 \approx \{f(\alpha)\}^{-1}\left\{1+\frac{3}{8}\frac{1-p}{k}\frac{m(\alpha)}{f(\alpha)}\right\}, \quad k \gg 1, \qquad (1.21)$$

where $m(\alpha) \approx 1-3,4\alpha$ at $\alpha \ll 1$ and $m(\alpha) \approx \dfrac{1}{2\alpha^2}$ at $\alpha \gg 1$.

In the case of polycrystalline thin films the equations for resisitivity takes form

$$\rho_f/\rho_g \approx \frac{4}{3}\frac{1-p}{1+p}\frac{f(\alpha)}{k}\left[0,4228+\ln\frac{f(\alpha)^{-1}}{k}\right], \quad k \ll 1. \quad (1.22)$$

For temperature coefficient of resistance the linearized expression takes the following form:

$$\beta d = \beta_g d - \beta_g \lambda_0 (1-p)H(\alpha);$$
$$\frac{\beta_g}{\beta_0} \approx 1+\frac{g(\alpha)}{f(\alpha)}, \qquad (1.23)$$

where $\beta_g$ is the temperature coefficient of resistance of bulk polycrystalline material, $H(\alpha)$ is tabulated function: $H(0) = 0.370$, $H(10) = 0.022$.

The procedure for determining the electrical parameters is as follows:

1) the equation (1.23) is straight-line equation $\beta d = Ad - B$; therefore plot the graph $\beta d$ versus $d$ (Fig. 1.8a);

2) the value of $\beta_g$ may be calculated from the slope of the linear law ($\beta d, d$);

3) taking into account that $\dfrac{\beta_g}{\beta_0} \approx 1+\dfrac{g(\alpha)}{f(\alpha)} = f(\alpha)$ at $\alpha \le 10$, the value of $\alpha$ may be calculated from equation (1.14);

20

4) the ordinate intercept is value of $B = \beta_g \lambda_0 (1 - p) H(\alpha)$, where the value of function $H(\alpha)$ can be measured on the plot $H(\alpha)$ versus $\alpha$ (Fig. 1.8 b).
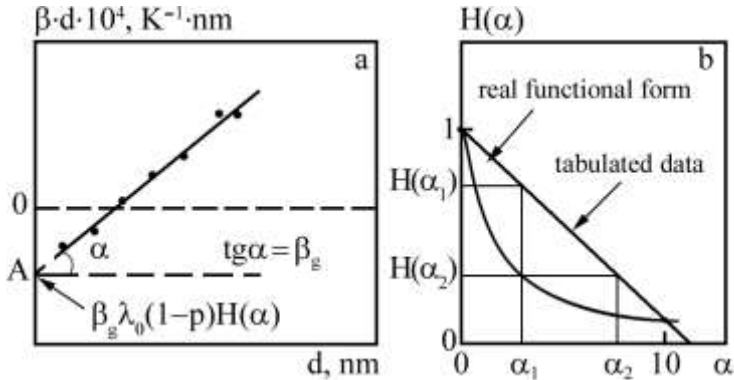


Figure 1.8 − Procedure for the determination of the electrical parameters in the framework of the lianearized model: dependences $\beta d$ versus $d$ (a) and $H(\alpha)$ versus $\alpha$ (b)

The main disadvantage of linearized model lies in the fact that it can be used in the case $L < d$ only. Besides, this model is not effective at interpretation of external size effect. In some cases, the calculation value of the specularity parameter by the equation (1.22) is less than 0, i. e. $p < 0$, that is non-physical result. The main mistake of linearized model is that the dependence $H$ versus $\alpha$ is a linear plot.

### 1.6.3 Model of isotropic scattering

Next alternative procedure of simplification of MS model is presented in the framework of the isotropic scattering. Model of isotropic scattering constitutes convenient treatment of the transport phenomena in both $L < d$ and $L > d$ cases and allows to perform separate experimental determination of the

parameters $p$, $r$ and $R$. This model describes size dependence of resistivity and temperature coefficient of resistance for polycrystalline thin film in assumption that the conditions for isotropic grain boundary scattering are satisfied. Under this assumption the total mean free path describing the effects of simultaneous background ($\lambda_0$), external surface ($\lambda_s$) and isotropic-grain-boundary ($\lambda_i$) scattering processes may be written as

$$\lambda^{-1}(\theta) = \lambda_0^{-1} + \lambda_i^{-1} + \lambda_s^{-1}, \qquad (1.24)$$

where the mean free path related to the isotropic grain boundary scattering is

$$\lambda_i^{-1} = A \cdot D_g^{-1} \ln \frac{1}{t}, \qquad (1.25)$$

where $A$ is the coefficient of isotropic grain boundary scattering to be determined, $D_g$ is the grain diameter, $R$ is the specular reflection parameter at the grain boundaries.

The problem of determining functional dependence $\rho(d)$ is treated by using the Boltzmann's equation and calculation of the current density $J(z)$ across the thickness. After some mathematical manipulation the main expression of the isotropic scattering model takes form:

$$\sigma_{fp}/\sigma_0 = \frac{3}{4} \int_0^\pi \frac{\sin^3 \theta}{1 + A\lambda_0 D_g^{-1} \ln \frac{1}{t} + d^{-1}\lambda_0 \ln \frac{1}{p}|\cos \theta|} d\theta, \quad (1.26)$$

$$\sigma_{fp}/\sigma_0 = \frac{3}{2\mu}\left( \alpha - \frac{1}{2} + \left(1 - \alpha^2\right)\ln\left(1 + \alpha^{-1}\right) \right) \qquad (1.27)$$

22

with $\alpha = \mu^{-1}\left(1 + AD_g^{-1}\lambda_0 \ln\dfrac{1}{p}\right) = \mu^{-1}\left(1 + Av^{-1}\right)$.

The linearized expression for the reduced TCR and the equation for calculation grain boundary TCR $\beta_g$ are

$$\beta^{-1}d = \beta_g^{-1}d + \frac{3}{8}\frac{\lambda_0}{\beta_0}\ln\frac{1}{p}, \qquad (1.28)$$

$$\beta_g \beta_0^{-1} = \left[1 + 1{,}45\frac{\lambda_0}{L}\ln\left(\frac{1}{r}\right)\right]^{-1}, \qquad (1.29)$$

where $r$ is the transmission parameter.

Taking into account that

$$\frac{R}{(1-R)} = 0{,}97\ln\left(\frac{1}{r}\right), \qquad (1.30)$$

equations (1.28) and (1.29) allow to calculate the electrical parameter by the next procedure:

1) the linearized expression for the reduced TCR (1.28) is strain lain equation $\beta^{-1}d = Ad + B$ which may be plotted as a dependence $\beta d^{-1}$ versus $d$ (Fig. 1.9 a);

2) the value of $\beta_g$ may be calculated from the slope of the linear law $(\beta^{-1}d, d)$;

3) from the ordinate intercept $A = \dfrac{3}{8}\dfrac{\lambda_0}{\beta_0}\ln\dfrac{1}{p}$ and tabulated values of $\beta_0$ and $\lambda_0$ ($\rho_0 \cdot \lambda_0 = \text{const}$) the value of $p$ is then calculated;

4) from the equations (1.29) and (1.30) the values of $R$ and $r$ are then calculated for different values of the average grain parameters in order to obtain size dependence of the grain size (1.9 b).

$\beta^{-1} \cdot d \cdot 10^{-4}$, K$^{-1} \cdot$nm

a

$\mathrm{tg}\alpha = \beta_g^{-1}$

B

$\alpha$

$\dfrac{3}{8} \dfrac{\lambda_0}{\beta_0} \ln\dfrac{1}{p}$

d, nm

L, nm

b

d, nm
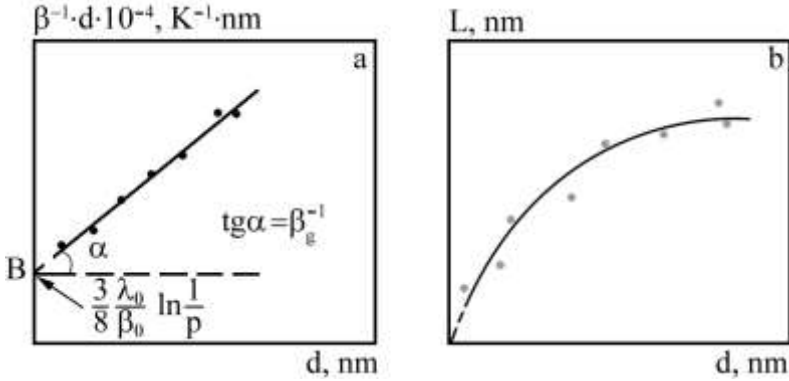
Figure 1.9 − Procedure for the electrical parameters determination in the framework of the isotropic scattering model: dependence $\beta d^{-1}$ versus $d$ (a) and size dependence of the average grain size (b).

### 1.6.4 Three-dimensional model

Three-dimensional model assumes that the grain boundaries in polycrystalline films can be represented by three arrays of "planar type" potentials with rough surfaces oriented perpendicular to the $x$-, $y$- and $z$ axes respectively. These planes are geometrically defined by an average interplanar spacing, $D_g$. In the case of polycrystalline films, the current is due to electrons which have been transmitted through a large number of grains, so that the associated mean free path can be statistically calculated by identifying the average grain diameter with $D_g$. It is the reason why only regular arrays of grain boundaries are considered in the rest of the section.

Starting from the Boltzmann formulation of the distribution functions of electrons when both background scattering and grain boundary scattering are operative, the conductivity $\sigma_g$ of a film subjected to an electric field applied in the $x$-direction is found to be

24

$$\sigma_g = \frac{3}{4\pi}\sigma_0 \int\limits_0^{2\pi} d\phi \int\limits_0^{\pi} \frac{\sin^3\theta\cos^2\phi}{1+\lambda_0\lambda_g^{-1}}d\theta, \qquad (1.31)$$

where $\theta$ and $\varphi$ are polar coordinates.

In general case the equation of the reduced conductivity is the following:

$$\sigma_g \big/ \sigma_0 = G(v) = \frac{3}{2b_{3\infty}}\left\{ a_{3\infty} - \frac{1}{2} + \left(1-a_{3\infty}^2\right)\ln\left(1+a_{3\infty}^{-1}\right) \right\} \qquad (1.32)$$

with $b_{3\infty} = (1-C)\cdot v^{-1}$, $a_{3\infty} = \left(1+C^2 v^{-1}\right)b_{3\infty}^{-1}$,
where $C = 4/\pi$,

$$v = \frac{L}{\lambda_0}\cdot\left(\ln\frac{1}{r}\right)^{-1}, \qquad (1.33)$$

$$\mu = \frac{d}{\lambda_0}\left(\ln\frac{1}{p}\right)^{-1}. \qquad (1.34)$$

In the case when $r=1$, $d/\lambda_0 \ll 1$, $p<1$ after mathematical manipulation one finds the expressions for the TCR of the polycrystalline ($\beta_p$) and the monocrystalline ($\beta_m$) films respectively in most general form:

$$\frac{\beta_p}{\beta_0} = \frac{a_p}{1+c^2\cdot v^{-1}}\cdot\frac{V(a_p)}{U(a_p)}, \qquad (1.35)$$

$$\frac{\beta_m}{\beta_0} = \frac{a_m}{1+c^2\cdot v^{-1}}\cdot\frac{V(a_m)}{U(a_m)}, \qquad (1.36)$$

where $a_p = \left(1+c^2\cdot v^{-1}\right)\cdot b_p^{-1}$, $a_m = \left(1+c^2\cdot v^{-1}\right)\cdot b_m^{-1}$, $V(a_p)$ and $U(a_p)$ are known function.

25

In the case of monocrystalline thin film the linearized expression for the TCR takes form

$$\left(\beta_m \ln \frac{\lambda_0}{d}\right)^{-1} = \beta_0^{-1}\left(1+c^2\cdot v^{-1}\right)\left[1+\left(\ln \frac{\lambda_0}{d}\right)^{-1}\ln\frac{\ln(1/p)}{1+c^2\cdot v^{-1}}\right].$$

(1.37)

In the case of polycrystalline thin film the linearized expression for the TCR takes form

$$\left(\beta_p \ln \frac{\lambda_0}{d}\right)^{-1} = 1,45\beta_0^{-1}\left(1+c^2\cdot v^{-1}\right)\left[1+\left(\ln \frac{\lambda_0}{d}\right)^{-1}\ln\frac{\ln(1/p)}{1+c^2\cdot v^{-1}}\right].$$

(1.38)

To determine the electrical parameters in the framework of the three-dimensional model it is necessary to complete the next procedure:

1) the linearized expressions for the reduced TCR (1.37) and (1.38) are the strain lain equations $\left(\beta_m \ln \frac{\lambda_0}{d}\right)^{-1} = A + B\left(\ln \frac{\lambda_0}{d}\right)^{-1}$,

and $\left(\beta_p \ln \frac{\lambda_0}{d}\right)^{-1} = C + D\left(\ln \frac{\lambda_0}{d}\right)^{-1}$ respectively. Hence, plot the

graph $\left(\beta_m \ln \frac{\lambda_0}{d}\right)^{-1}$ versus $\left(\ln \frac{\lambda_0}{d}\right)^{-1}$ in the case of the

monocrystalline film or $\left(\beta_p \ln \frac{\lambda_0}{d}\right)^{-1}$ versus $\left(\ln \frac{\lambda_0}{d}\right)^{-1}$ in the case

of the polycrystalline film (Fig. 1.10);

2) the value of $\beta_m$ ($\beta_p$) may be calculated from the slope of the graph;

3) from the ordinate intercept A(B) and tabulated value of $\beta_0$ the value of $v$ is then calculated;
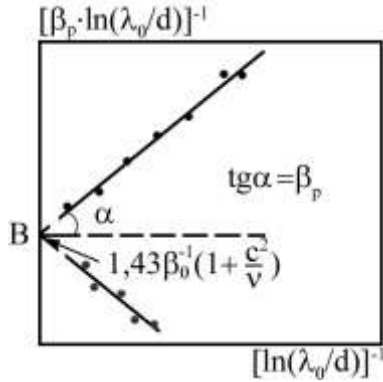
Figure 1.10 − Procedure for electrical parameters determination in the framework of three-dimensional model (case of the polycrystalline film)

4) from the equations (1.34) and tabulated value of $\lambda_0$ ($\rho_0 \cdot \lambda_0 =$ const) the value of $r$ is then calculated.

### 1.7 Interpretation of experiments

Measurements of the resistivity and the temperature coefficient of resistance on metal thin films are widely presented in the literature. The interpretation of experimental data in the term of approximation relationships of Tellier, Tosser and Pichard such as the linearized model, the model of isotropic scattering and the three-dimensional model is presented in this section.

The experimental size dependences of resistivity and TCR for different thin films are presented in Fig. 1.11 and 1.12, respectively. From the practical point of view, the resistivity data are more convenient than the TCR data because of the inaccuracy in the TCR, mainly due to its low value. So, as attempted, the results from the TCR data will be presented then.
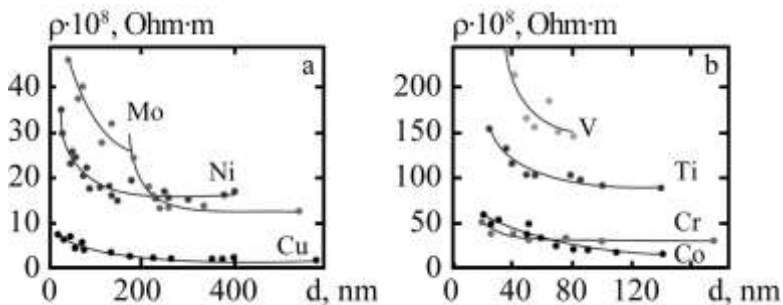
Figure 1.11 – Size dependences of the resistivity for thin films Ni, Cr (a), Sc, V (b), Cu, Mo (c), Co, Ti (d)
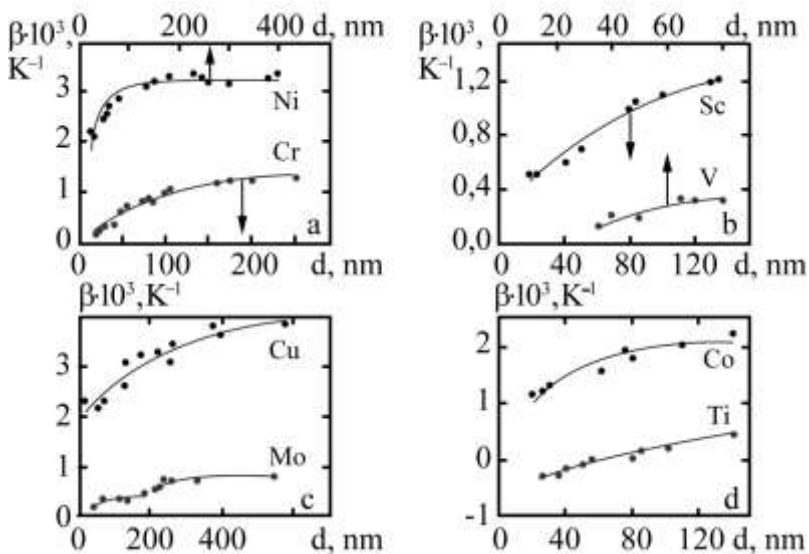


Figure 1.12 – Size dependences of TCR for thin films Ni, Cr (a), Sc, V (b), Cu, Mo (c), Co, Ti (d)

28

Table 1.1 – Numerical values of electrical parameters obtained on the base of approximation relationships of Tellier, Tosser and Pichard

| Film | $d$, nm | Linearized model | | | Model of isotropic scattering | | | Three-dimensional model | | |
|---|---|---|---|---|---|---|---|---|---|---|
| | | $\beta_\infty \cdot 10^{-3}$, $K^{-1}$ | $\lambda(1-p)$, nm | $R$ | $p$ | $R$ | $r$ | $p$ | $R$ | $r$ |
| Cu | > 180 | 4,1 | 83,0 | 0,11 | 0,14 | 0,05 | 0,93 | 0,001 | – | 0,80–0,72 |
| Cu | < 100 | – | 38,7 | 0,35–0,42 | 0,09 | 0,18–0,25 | 0,81–0,72 | | | |
| Ni | 10–400 | 3,94 | 32,0 | 0,31–0,75 | 0,08 | 0,22–0,70 | 0,70–0,10 | – | – | – |
| Sc | 20–140 | 1,57 | 35,1 | 0,39–0,49 | 0,04 | 0,37–0,47 | 0,54–0,40 | 0,01 | 0,49 | 0,43 |
| Cr | 20–140 | 1,52 | 34,2 | 0,03–0,15 | 0,04 | 0,02–0,14 | 0,98–0,85 | 0,01 | – | 0,99–0,93 |
| Co | 20–90 | 2,50 | 36,5 | 0,13–0,41 | 0,05 | 0,12–0,46 | 0,87–0,53 | 0,001 | – | 0,99–0,87 |
| Al | < 600 | 1,10 | 31,0 | 0,44 | 0,59 | 0,48 | 0,52 | 0,50 | – | 0,50 |
| Zn | < 900 | 1,92 | 12,0 | 0,52 | 0,59 | 0,64 | 0,36 | 0,50 | – | 0,43 |

Any experimental data for the TCR can be presented as linear low (1.23), (1,28) and (1.38) and interpreted from either the linearezed model or the model of isotropic scattering model or three-dimensional model. Results of electrical parameter calculation are presented in the Table 1.1.

As conclusion, it can be noted, that the specularity parameter $p$ takes values in the range from 0.001 to 0.6 and both the reflection parameter $R$ and the transmission parameter $r$ take values 0.2–0.9.

The grain boundary is energy barrier for conduction electrons. In this point of view, taken into account the energy value which charge carrier failed at transmission through the grain boundary, grain boundaries could be of three types:
– barrier type ($r = 0.2$–$0.3$);
– transparent for conduction electrons ($0.3 \leq r \leq 0.8$);
– nontransparent for conduction electrons ($r = 0.8$–$0.9$).

### 1.8 Problems

### Problem # 1
Re-arrange equation $\dfrac{1-p}{1+p}$ to the form $\dfrac{1}{1+2p}$.

### Problem # 2
What is the physical nature of size effect in conductivity of thin film?

### Problem # 3
Under the experimental results for scandium thin films (Fig. 1.13) determine the value of $\rho_\infty$ and $\lambda_0$ in diffusive approach ($p = 0$).

$\rho \cdot 10^6$, Ohm·m

T = 300 K

d, nm
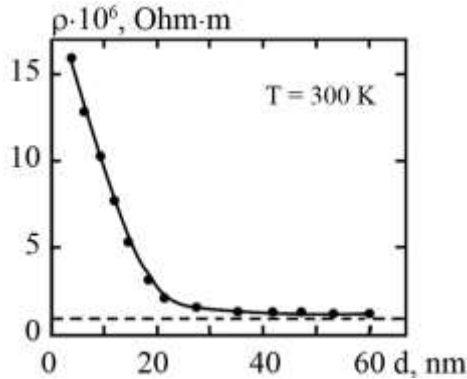
Figure 1.13 – The experimental dependence of $\rho$ compared to $d$ for scandium thin films, which have been prepared in vacuum $10^{-7}$ Pa

**Problem # 4**

Compare the value of $\rho_\infty$, which has been received in the previous exercise with value of $\rho_0(300\ \text{K}) = 7{,}5 \cdot 10^{-7}$ Ohm·m for bulk materials. Explain the reason of difference.

**Problem # 5**

Explain why the values $p < 0$ and $p > 0$ do not have physical meaning. What is the physical meaning of the parameter $p = 0$?

**Problem # 6**

On the basis of the definition of temperature coefficient of resistance (TCR) $\beta = \dfrac{1}{\rho} \cdot \dfrac{\partial \rho}{\partial T}$ or $\beta_\infty = \dfrac{1}{\lambda_0} \cdot \dfrac{\partial \lambda_0}{\partial T}$ show that

from the equation $\dfrac{\rho}{\rho_\infty} \cong 1 + \dfrac{3}{8} \cdot \dfrac{\lambda_0(1-p)}{d}$ one can receive such

equation for TCR: $\dfrac{\beta}{\beta_\infty} \cong 1 - \dfrac{3}{8} \cdot \dfrac{\lambda_0(1-p)}{d}$ .

*Directive: It is necessary to use the expansion procedure on binomial theorem* $(a+x)^n \cong a + nx + ...,$ *where* $x \ll a.$

### Problem # 7

Show that equation $\dfrac{\beta}{\beta_0} \cong \left[ 1 + \dfrac{3}{8} \dfrac{\lambda_0(1-p)}{d} f(\alpha) \right]^{-1} \cdot f(\alpha)$

can        be        obtained        from        equation

$\dfrac{\beta}{\beta_0} = \left[ 1 + \dfrac{3}{8} \dfrac{\lambda_0(1-p)}{d} f(\alpha) \right]^{-1} \cdot \left[ 1 + \alpha \dfrac{df/d\alpha}{f(\alpha)} \right]$ at the condition

$\dfrac{3}{8} \dfrac{\lambda_0(1-p)}{d} \ll 1$ .

### Problem # 8

Create graph of the function $f(\alpha)$ vs the value of $\alpha$, which changed in the range from 0,01 to 10.

### Problem # 9

Explain a physical meaning of parameters: $\rho_g$, $\beta_g$, $R$ and $r$. Compare the physical meaning of $\rho_g$ and $\rho_\infty$.

### Problem # 10

On the basis of experimental data for scandium thin films at 300 K (Fig 1.14) calculate parameters $R$ and $r$ in the frame of effective mean free path model and model of isotropic scattering. Take value of mean free path $\lambda_0$ from exercise # 3.

**Problem # 11**

Explain why the value of $R + r$ is unequal to one according to result of exercise # 10.
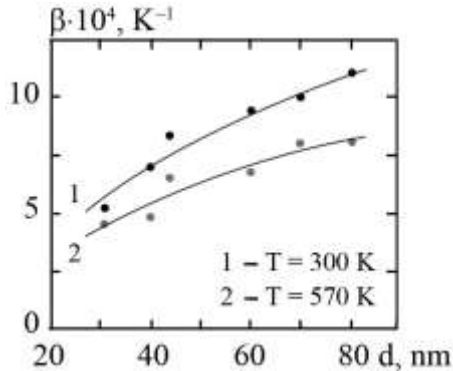


Figure 1.14 – Size dependence of TCR for scandium thin film at $T = 300$ (1) and 570 K (2)

**Problem # 12**

The process of impurity atom grain boundary diffusion occurs in scandium thin films. On the basis of data presented at the Figures 1.13 and 1.14 plot dependence of resistivity and temperature coefficient of resistance vs film thickness at different values of $\gamma \cdot c$ (the parameter of grain boundary scattering at low concentration of impurity atom is directly proportional to impurity atom concentration i. e. $R' = R \pm \gamma \cdot c$, where $R'$ and $R$ are parameters of the specular reflection at the grain boundaries at $c \neq 0$ and $c = 0$, respectively; $c$ is concentration of impurity atom; $\gamma$ is aspect ratio). Examine the cases $\gamma < 0$ and $\gamma > 0$.

The value of $\rho_0(300) = 75 \cdot 10^{-8}$ Ohm·m, $\beta_0(300) = 42{,}5 \cdot 10^{-4}$ K$^{-1}$, $\lambda_0(1-p)$ (300) = 130 nm and $L \cong d$ in the range of the thickness 50–100 nm.

Note, the values of $\rho_g$ and $\beta_g$ can be calculated by extrapolation of dependences $\rho = \rho(d^{-1})$ and $\beta = \beta(d^{-1})$ to zero (Fig. 1.15).
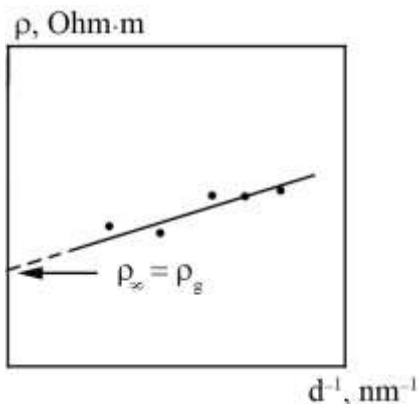


Figure 1.15 – The method of $\rho_g$ value determination by extrapolation to zero of experimental dependence $\rho$ vs inverse thickness

### Problem # 13

Calculate the size dependence of ratio $\rho/\rho_g$ at different values of parameter $\gamma \cdot c$, using the data presented in the Table 1.2. Examine the cases $\gamma < 0$ and $\gamma > 0$. The value of $\rho_0(300) = 1,3 \cdot 10^{-7}$ Ohm·m, $\rho_g(300) = 2,6 \cdot 10^{-7}$ Ohm·m.

Table 1.2 – Electrophysical properties of chromium thin films

| $d$, nm | $\lambda_0(1-p)$, nm | $L$, nm | $R$ | $d$, nm | $\lambda_0(1-p)$, nm | $L$, nm | $R$ |
|---|---|---|---|---|---|---|---|
| 50 | 131 | 25 | 0,09 | 80 | 140 | 40 | 0,16 |
| 60 | 130 | 30 | 0,11 | 90 | 131 | 45 | 0,20 |
| 70 | 139 | 35 | 0,14 | 100 | 127 | 50 | 0,24 |

## 1.9 References

1. Басов А. Г. Електрофізичні властивості та кристалічна структура плівок алюмінію / А. Г. Басов, А. О. Степаненко, А. М. Чорноус // Вісник СумДУ. – 2005. – Т. 80, No. 8. – С. 170–176.

2. Білоус О. А. Електрофізичні властивості плівок молібдену в умовах внутрішнього розмірного ефекту / О. А. Білоус, А. М. Чорноус // ВАНТ. Серия: Вакуум, чистые материалы, сверхпроводники. – 2003. – No. 5. – С. 146–151.

3. Пазуха І. М. Фізичні властивості плівкових матеріалів мікро- і наноелектроніки : навчальний посібник / І. М. Пазуха, І. Ю. Проценко, І. В. Чешко ; за заг. ред. І. Ю. Проценка. – Суми : Сумський державний університет, 2014. – Ч. 1. – 230 с.

4. Проценко І. Ю. Тонкі металеві плівки (технологія та властивості) : навчальний посібник / І. Ю. Проценко, В. А. Саєнко. – Суми : Сумський державний університет, 2002. – 187 с.

5. Комник Ю. Ф. Физика металлических пленок / Ю. Ф. Комник. – Москва : Атомиздат, 1979. – С. 90–102.

6. Лобода В. Б. Исследование электрических свойств тонких пленок хрома и скандия / В. Б. Лобода, И. Е. Проценко, В. Г. Шамоня // УФЖ. – 1982. – Т. 27, No. 9. – С. 1343–1349.

7. Проценко И. Е. Расчет параметров электропереноса тонких поликристаллических пленок металлов / И. Е. Проценко // Изв. вузов. Физика. – 1988. – No. 6. – С. 42–47.

8. Bakonyi I. Electrodeposited multilayer films with giant magnetoresistance (GMR): progress and problems / I. Bakonyi, I. Peter // Progress in Mater. Sci. – 2010. – Vol. 53. – P. 107–245.

9. Chornous A. M. Experimental test of a three-dimensional model for electrophysical properties of metal films / A. M. Chornous, N. M. Opanasiuk, A. D. Pogrebniak, I. Yu. Protsenko // Jpn. J. Appl. Phys. – 2000.– Vol. 39, No. 12B. – P. L1320–L1323.

10. Current-Driven Magnetization reversal and spin-wave excitations in Co/Cu/Co pillars / J. A. Katine, F. J. Albert, R. A. Buhrman et al. // Phys. Rev. Lett. – 2000. – Vol. 84. – P. 3149–3152.

11. Ghosh C. K. Electrical resistivity and galvanomagnetic properties of evaporated nickel films / C. K. Ghosh, A. K. Pal // J. Appl. Phys. – 1980. – Vol. 51. – P. 2281–2285.

12. Kondrakhova D. M. Thin film systems based on Co and Cr Or Cu: magnetoresistive properties and application / D. M. Kondrakhova, I. M. Pazukha, I. Yu. Protsenko // Univ. J. Phys. and Appl. – 2014. – Vol. 2, No. 2. – P. 85.

13. Luby S. Pseudo spin-valve with different spacer thickness as sensing elements of mechanical strain / S. Luby, B. Anwarzai, V. Ac, E. Maikova, R. Senderak // Vacuum. – 2012. – Vol. 86. – P. 718.

14. Mayadas A. F. Electrical-resistivity model for polycrystalline films: the case of arbitrary reflection at external surfaces / A. F. Mayadas, M. Shatzkes // Phys. Rev. B. – 1970. – Vol. 1. – P. 1382–1383.

15. Morley N. A. Magnetoresistance measurements on Fe/Si and Fe/Ge multilayer thin films / N. A. Morley, M. R. J. Gibbs, K. Fronc, R. Zuberek // J. Magn. Magn. – 2005. – Vol. 286. – P. 91.

16. Parkin S. S. P. Magnetic domain-wall racetrack memory / S. S. P. Parkin, M. Hayashi, L. Thomas // Science. – 2008. – Vol. 320. – P. 190.

17. Pazukha I. M. Fe/Cr and Cu/Cr Film Pressure-Sensitive Elements / I. M. Pazukha, I. E. Protsenko // Tech. Phys. – 2010. – Vol. 80, Issue 4. – P. 140–144.

18. Pichard C. R. Statistical model of electrical conduction in polycrystalline metals / C. R. Pichard, C. R. Tellier, A. J. Tosser // Thin Solid Films. – 1979. – Vol. 62. – P. 189–194.

19. Suri R. Electron transport properties of thin copper films / R. Suri, A. P. Thakoor, K. L. Chopra // J. Appl. Phys. – 1975. – Vol. 46. – P. 2574–2581.

20. Tellier C. R. A theoretical description of grain boundary electron scattering by an effective mean free path / C. R. Tellier // Thin Solid Films. – 1978. – Vol. 51. – P. 311–317.

21. Tellier C. R. Physical bases of Warkusz's equation for polycrystalline metallic conductivity / C. R. Tellier, A. J. Tosser // J. Electrocomp. Sc. Technol. – 1980. – Vol. 6. – P. 91–92.

22. Tellier C. R. Size effects in thin films / C. R. Tellier, A. J. Tosser. – New York : Elsevier, 1982. – 310 p.

23. Tosser A. J. Thin polycrystalline metallic-film conductivity under the assumption of isotropic grain-boundary scattering / A. J. Tosser, C. R. Tellier, C. R. Pichard // J. Mat. Sci. – 1981. – Vol. 16. – P. 944–948.

24. Tyschenko K. V. Electrophysical properties on nanocrystalline platinum thin films / K. V. Tyschenko, I. M. Pazukha, T. M. Shabelnyk, I. Yu. Protsenko // J. Nano-Electron. Phys. – 2013. – Vol. 5, No. 1. – P. 01029–1–01029–5.

25. Tyschenko K.V. Nonlinear effects in strain properties of thin film alloys on the base of Fe and Ni / K. V. Tyschenko, I. Yu. Protsenko // Metallofiz. Noveishie Technol. – 2012. – Vol. 34. – P. 907.

26. Vorobiov S. I. Sensitive element of the magnetic field sensor based on three-layer film system Co/X/Co (X = Dy, Gd) / S. I. Vorobiov, O. V. Shutylieva, I. M. Pazukha,

A. M. Chornous // Tech. Phys. – 2014. – Vol. 84, No. 11. – P. 66–71.

27. Zhang Q. G. Influence of grain boundary scattering on the electrical properties of platinum nanofilms / Q. G. Zhang, X. Zhang, B. Y. Cao // Appl. Phys. Lett. – 2006. – Vol. 89. – P. 114102.

# SECTION 2
## Size effects in electrical resistivity and TCR of double-layered films

### 2.1 Introduction

The theoretical models of size effect for double-layered films and their experimental approbation are presented in this section.

The main difference between size effect in thin films and in double-layered films is that in second case new mechanism of the conduction electron scattering appears. This mechanism is scattering of charge carrier at the boundary between two layers, which are called an interface scattering. Besides, both layers are characterized by their own mean free path $\lambda_{01}$ and $\lambda_{02}$, as well as the linear coefficients of thermal expansion $\alpha_1$ and $\alpha_2$. Thickness relation is also significant too as the internal and external size effects appear separately in each layer.

### 2.2 The geometry of double-layered films

The double-layered thin film consists of upper layer of a metal 1 with thickness $d_1$ and average grain size $L_1$ and lower layer of a metal 2 with thickness $d_2$ and average grain size $L_2$. The sample is subjected to an electrical field $E$ in the $x$ direction. The geometry of the film system is presented in Fig. 1.12.

There are three scattering mechanisms for conduction of electrons in such a structure: scattering at the external surfaces, at the grain boundaries and at the interface between the layers. The first mechanism is described by the specularity parameters $p_1$ and $p_2$ related to lower and upper layers respectively. The second mechanism is characterized by two

parameters: the specular reflection at the grain boundaries $R_1$ and $R_2$ and the transmission parameter across the grain boundaries $r_1$ and $r_2$.
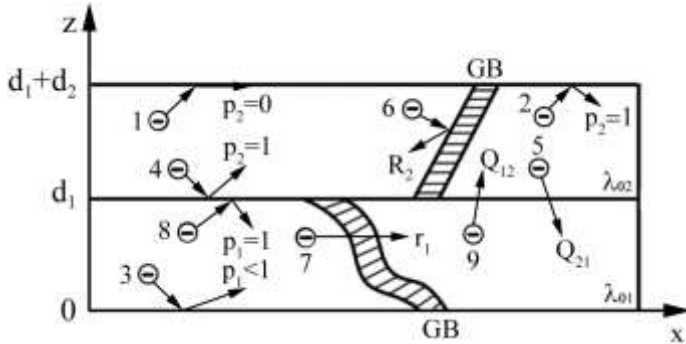


Figure 2.1 – The geometry of double-layered thin film

Indexes 1 and 2 are related to lower and upper layers respectively. The third mechanism is described by the parameter of interface scattering $Q$, which defines the probability of electron reflection at the interface or transmission across the interface from upper to lower layer ($Q_{21}$) and from lower to upper layer ($Q_{12}$)).

For a theoretical analysis, it is assumed that both metals have isotropic bulk mean free paths $\lambda_{01}$ and $\lambda_{02}$ and that the Fermi energies of two metals are sufficiently close and that the contact potential difference arising at the interface may be neglected.

Thus, for a theoretical analysis of the experimental data, some models have been proposed.

## 2.3 The Dimmich model

The Dimmich model describes the electrical conduction and TCR for double-layered films. Dimmich has proposed

double-layered model for the electrical conductivity and the TCR taking into account the mechanisms of electron scattering at external surfaces of the films, grain boundaries, interface between the layers and the isotropic background scattering due phonons and point defects.

The distribution function $f(\upsilon, z)$ for the charge carrier for the sample in the electrical field can be given as

$$
\begin{aligned}
f(\upsilon, z) &= f_0 + f_1(\upsilon, z), \\
f(\upsilon, z) &= f_0 + f_2(\upsilon, z),
\end{aligned}
\tag{2.1}
$$

where $f_0$ is the equilibrium distribution, $f_1(\upsilon, z)$ and $f_2(\upsilon, z)$ are the deviations from the Fermi-Dirac function induced by the electrical field $E$ in the layers $-d_1 \le z \le 0$ and $0 \le z \le d_2$ respectively, $\upsilon$ is the electron velocity.

The Boltzmann kinetic equations for the layers take the forms

$$
\frac{\partial f_1}{\partial z} + \frac{f_1}{\tau_1^* \upsilon_z} = \frac{eE}{m_1^* \upsilon_z} \frac{\partial f_0}{\partial \upsilon_x},
\tag{2.2}
$$

$$
\frac{\partial f_2}{\partial z} + \frac{f_2}{\tau_2^* \upsilon_z} = \frac{eE}{m_2^* \upsilon_z} \frac{\partial f_0}{\partial \upsilon_x},
$$

where $\tau_1^*$ and $\tau_2^*$ are the grain boundary limited relaxation times; $e$ is the electron charge; $m_1^*$ and $m_2^*$ are the effective electron masses for layers material 1 and 2 respectively.

The procedure of obtaining general expression for the ratio of conductivity of the layer $\sigma_i$ to the value of conductivity $\sigma_{0i}$ in the bulk monocrystalline material, where $i = 1$ or 2 is number of layer, is presented in the work in detail.

General expressions take form:

$$\frac{\sigma_1}{\sigma_{01}} = F(\beta_1) - \frac{3}{\pi k_1} \int\limits_0^{\pi/2} d\phi \int\limits_1^\infty dt \left( \frac{1}{t^3} - \frac{1}{t^5} \right) \times$$

$$\times \frac{\cos^2 \phi \{1 - \exp(-tH_1 k_1)\}}{H_1^2 G} B_1, \qquad (2.3)$$

$$\frac{\sigma_2}{\sigma_{02}} = F(\beta_2) - \frac{3}{\pi k_2} \int\limits_0^{\pi/2} d\phi \int\limits_1^\infty dt \left( \frac{1}{t^3} - \frac{1}{t^5} \right) \times$$

$$\times \frac{\cos^2 \phi \{1 - \exp(-tH_2 k_2)\}}{H_2^2 G} B_2, \qquad (2.4)$$

where $B_1$, $B_2$, $G$, $H_1$, $H_2$ are the functions presented in Dimmich work.

As noticed in previous section, the resistivity data are more convenient than the TCR data from the practical point of view, so in the framework of Dimmich model is considered the dependence of TCR from thicknesses $d_1$ and $d_2$.

Temperature coefficient of resistance $\beta$ is relative change of the resistivity at temperature change upon 1 K, i. e.

$$\beta = \frac{1}{\rho} \frac{d\rho}{dT} = \frac{d \ln \rho}{dT} .$$

The double-layered film can be presented as two films in parallel connected resistors. The total value of such system resistance is calculated as $R = R_1 \cdot R_2 / (R_1 + R_2)$. Taking into account that $\rho_i = R_i \frac{a \cdot d_i}{l}$, where $i = 1, 2$ is number of the layer, equation for the total system resistivity takes form $\rho = \frac{\rho_1 \rho_2 (d_1 + d_2)}{\rho_1 d_2 + \rho_2 d_1}$. Thus, the equation for the TCR can be rewritten as

$$\beta = \frac{d \ln \rho}{dT} = \frac{d \ln \left( \dfrac{\rho_1 \rho_2 (d_1 + d_2)}{\rho_1 d_2 + \rho_2 d_1} \right)}{dT}.$$

Using the general equations (2.3) and (2.4) for the electrical conductivity, differentiation yields the general expression for the TCR in the form

$$\beta = A_1 \left\{ \begin{array}{l} \beta_{01} \left( 1 - \dfrac{d \ln F_1}{d \ln k_1} - \dfrac{d \ln F_1}{d \ln m_1} + \dfrac{d \ln F_1}{d \ln a} \right) - \\ - \beta_{02} \left( \dfrac{d \ln F_1}{d \ln k_2} + \dfrac{d \ln F_1}{d \ln m_2} + \dfrac{d \ln F_1}{d \ln a} \right) \end{array} \right\} +$$
$$+ A_2 \left\{ \begin{array}{l} \beta_{02} \left( 1 - \dfrac{d \ln F_2}{d \ln k_2} - \dfrac{d \ln F_2}{d \ln m_2} - \dfrac{d \ln F_2}{d \ln a} \right) - \\ - \beta_{02} \left( \dfrac{d \ln F_2}{d \ln k_1} + \dfrac{d \ln F_2}{d \ln m_1} - \dfrac{d \ln F_2}{d \ln a} \right) \end{array} \right\},$$

(2.5)

where $F = \dfrac{\rho_{0i}}{\rho_i}$ is the Fuch's function $(i = 1, 2)$,

$A_1 = \dfrac{d_1 \sigma_{01} F_1}{d_1 \sigma_{01} F + d_2 \sigma_{02} F}$, $\qquad A_2 = \dfrac{d_2 \sigma_{02} F_2}{d_1 \sigma_{01} F + d_2 \sigma_{02} F}$, $\qquad \sigma = 1/\rho$,

$a = \lambda_{01} H_2 m_2^* \left( \lambda_{02} H_1 m_1^* \right)^{-1}$, $m^*$ is the effective electron mass, $k_i = d_i / \lambda_{0i}$ is the reduced thickness, $l_i = L_i / \lambda_{0i}$ is the reduced grain size, $H_i = H_i(\alpha, \varphi)$, $\alpha = \dfrac{\lambda_0}{L} \dfrac{1}{R(1-R)}$, $\varphi$ is the approached angle to the grain boundary.

The mathematical form of equation (2.5) is not very favourable to an easy numerical evaluation of the film TCR so

Protsenko I. Yu. et al. have been proposed the method of simplification equation (2.5). According to Protsenko I. Yu. et al. at assumption that: $d\ln F_i/d\ln a = 0$, where $a$ is thickness independent parameter ($a = $ const); $d\ln F_i/d\ln k_k \approx 0$, $d\ln F_i/d\ln l_k \approx 0$ ($i \neq k$) in the case when the coefficient of interface scattering equals to 1 with $\lambda_{01} = \lambda_{02}$, or equals to 0, the equation (2.5) can be rewritten as

$$\beta = A_1\beta_{01}\left(1 - \frac{d\ln F_1}{d\ln k_1} - \frac{d\ln F_1}{d\ln l_1}\right) + A_2\beta_{02}\left(1 - \frac{d\ln F_2}{d\ln k_2} - \frac{d\ln F_2}{d\ln l_2}\right),$$

(2.5′)

where $\dfrac{d\ln F_1}{d\ln k_1} = d_1\left(\lambda_{01}F_1\right)^{-1}\dfrac{\partial F_1}{\partial k_1}$ was determined through the experimental parameters.

For thick films the equation (2.5′) is reduced to

$$\beta = A_1\beta_{01} + A_2\beta_{02}.$$ 

(2.5″)

The experimental results and calculated data based on the Dimmich model are presented in Table 2.1. The comparison between experimental values of the TCR and the values derived from equation (2.5′) show some difference.

There are two main reasons of deviation between experimental data and calculated values for the TCR. The first one is the process of interdiffusion which leads to changing the parameters of scattering at the interfaces and at the grain boundaries. The second one is the process of the thermal expression which leads to the film deformation and as a result to both increase and decrease of the resistivity and the TCR. The Dimmich model leaves out of account these effects.

It can be noted that the experimental data better agreed with calculated ones when the $\beta_0$ is changed to $\beta_g$.

Table 2.1 – The experimental and calculated values of TCR with the Dimmich model for double-layered film systems

| Film (d, nm) | $\beta_{exp} \cdot 10^3$, K$^{-1}$ | $\beta_{calc} \cdot 10^3$, K$^{-1}$ |
|---|---|---|
| Co(75)/Cr(55)/S | 2,60 | 1,56 |
| Co(80)/Cr(120)/S | 2,40 | 1,42 |
| Cr(25)/Co(35)/S | 1,30 | 0,75 |
| Cr(40)/Co(40)/S | 1,70 | 0,89 |
| Cr(80)/Co(55)/S | 2,08 | 1,84 |
| Co(25)/Ni(20)/S | 2,95 | 1,99 |
| Co(90)/Ni(30)/S | 3,20 | 1,76 |
| Co(100)/Ni(65)/S | 3,45 | 2,45 |
| Ni(55)/Co(20)/S | 3,60 | 1,20 |
| Ni(80)/Co(59)/S | 3,60 | 2,00 |
| Ni(140)/Co(60)/S | 3,83 | 2,13 |

Protsenko I. Yu. et al. have shown that deviation of experimental data with calculated ones in the frame of Dimmich model may amount 70 % depending on type of thin film system. But accounting temperature dependence of scattering parameters $p$ and $r$ leads to better agreement of experimental data with calculated ones in the frame of the Dimmich model. So Protsenko I. Yu. et al. have proposed a trilayered model in which the temperature effect on scattering parameters ($p$, $r$, $Q$) has been taken into account.

This model requires several assumptions in its formulation which are summarized here:

1) the trilayered film can be presented as two ones in parallel connected resistors; each layer is characterized by thickness $d_i$, value of mean free path $\lambda_{0i}$, effective specularity parameter $p_i$, transmission parameter across the grain boundaries $r_i$ and parameter of interface scattering $Q_{ij}$ (from $i$-layer to $j$-layer);

2) temperature effects in scattering parameters were taken into account by corresponding temperature coefficient of resistance:

$$\beta_{\lambda_{0i}} = -\frac{d \ln \lambda_{0i}}{dT}, \ \beta_{pi} = -\frac{d \ln p_i}{dT}, \ \beta_{ri} = -\frac{d \ln r_i}{dT} \ \text{and} \ P_i \cong p_i$$

$$\beta_{Q_{ij}} = -\frac{d \ln Q_{ij}}{dT};$$

3) transmission of electrons across the interface may occur between adjacent layers (from $i$-layer to $(i + 1)$ layer) or between several layers (e. g., from $i$-layer to $(i \pm 1)$ and $(i \pm 2)$ layers) depends on relationship between layer thickness $d_i$ and mean free path $\lambda_{0i}$;

4) the processes of diffuse and specular scattering at interfaces ($P_i \cong p_i$) and interlayer transition ($Q_{ij}$) are taken into account;

5) the values of $Q_{ij}$ and $\beta_{Q_{ij}}$ are approximately equal to $r_i$ and $\beta_{r_i}$.

The model is shown in Figure 2.2.

The trilayered film in the framework of this model can be presented as three ones in parallel connected resistors, so equation for the total system resistance may be written as

$$\frac{1}{R} = \frac{a}{l} \left( d_1 \sigma_{01} F_1 + d_2 \sigma_{02} F_2 + d_3 \sigma_{03} F_3 \right).$$

Logarithmic differentiation on the temperature of this equation gives

$$\beta = A_1 \left( \alpha_1 - \frac{\partial \ln \sigma_{01}}{\partial T} - \frac{\partial \ln F_1}{\partial T} \right) + ... + A_3 \left( \alpha_3 - \frac{\partial \ln \sigma_{03}}{\partial T} - \frac{\partial \ln F_3}{\partial T} \right),$$

(2.6)

where $\alpha_1 = \frac{d \ln l}{dT}$ is the temperature coefficient of thermal expansion (the value of $\alpha_1 \sim (10^{-5} - 10^{-6}) \ \text{K}^{-1}$).

46

Figure 2.2 – The geometry of trilayered thin film system: 1 and 1´´ are surface scattering (in general case $p_1 = p_2$); 2, 2´ and 2´´ are grain boundary scattering (in general case $r_1 \neq r_2 \neq r_3$); 3, 3´ and 3´´ are scattering at interface and transmission through interface ( $P_{12} \cong p_1$; $P_{23} \cong p_2$; $P_{32} \cong p_3$; $Q_{12} \cong Q_{21}$; $Q_{23} \cong Q_{32}$); 3, 3´ and 3´´ are interlayer transitions at the $\lambda_{0_{12}}$; 4 and 4´´ are interlayer transitions at the $\lambda_{0_{13}}$

For taking into account temperature effects in scattering parameters ($p$, $r$, $Q$) $F_i$, it is necessary to write parameters as function of $k_i$ and $m_i$ as

$$F_i = [k_i(\lambda_{0i}, d_i, p_i, Q_{i(i\pm1)}), m_i(\lambda_{0i}, L_i, r_i, Q_{i(i\pm1)});$$
$$k_{i\pm1}(\lambda_{0i\pm1}, d_{i\pm1}, p_{i\pm1}, Q_{(i\pm1)i}, m_{i\pm1}(\lambda_{0i\pm1}, L_{i\pm1}, r_{i\pm1}, Q_{(i\pm1)i})].$$

(2.7)

Note, that values of $k_i$ are determined by surface scattering and $m_i$ by grain boundary and interface scattering. In expanded form derivative $d \ln F_1/dT$ has the form

47

$$\frac{d\ln F_1}{dT} = \frac{\partial \ln F_1}{\partial \ln k_1}\frac{d\ln k_1}{dT} + \frac{\partial \ln F_1}{\partial \ln m_1}\frac{d\ln m_1}{dT} + \frac{\partial \ln F_1}{\partial \ln k_1}\frac{\partial \ln k_1}{\partial \ln p_1}\frac{d\ln p_1}{dT} +$$

$$+ \frac{\partial \ln F_1}{\partial \ln m_1}\frac{\partial \ln m_1}{\partial \ln r_1}\frac{d\ln r_1}{dT} + \frac{\partial \ln F_1}{\partial \ln k_1}\frac{\partial \ln k_1}{\partial \ln k_2}\frac{d\ln k_2}{dT} +$$

$$+ \frac{\partial \ln F_1}{\partial \ln m_1}\frac{\partial \ln m_1}{\partial \ln m_2}\frac{d\ln m_2}{dT} + \frac{\partial \ln F_1}{\partial \ln k_1}\frac{\partial \ln k_1}{\partial \ln Q_{12}}\frac{d\ln pQ_{12}}{dT} +$$

$$+ \frac{\partial \ln F_1}{\partial \ln k_1}\frac{\partial \ln k_1}{\partial \ln k_2}\frac{\partial \ln k_2}{\partial \ln p_2}\frac{d\ln p_2}{dT} + \frac{\partial \ln F_1}{\partial \ln m_1}\frac{\partial \ln m_1}{\partial \ln m_2}\frac{\partial \ln m_2}{\partial \ln r_2}\frac{d\ln r_2}{dT} +$$

$$+ \frac{\partial \ln F_1}{\partial \ln k_1}\frac{\partial \ln k_1}{\partial \ln k_2}\frac{\partial \ln k_2}{\partial \ln Q_{12}}\frac{d\ln Q_{12}}{dT}.$$

(2.8)

Substituting equations (2.8) and analogical equations for $F_2$ and $F_3$ into (2.7), we finally obtain the equation for temperature coefficient of resistance for trilayered system:

$$\beta = \sum_{i,j=1}^{3} A_i \left\{ \beta_{0i} - \left(1 - \frac{\beta_i}{\beta_{0i}}\right)\cdot\left(2\beta_{0i} + \beta_{pi}\cdot\frac{\partial \ln k_i}{\partial \ln p_i} + \beta_{ri}\cdot\frac{\partial \ln m_i}{\partial \ln r_i} + \right.\right.$$

$$+ \beta_{Q_{i(i\pm1)}}\cdot\frac{\partial \ln k_i}{\partial \ln Q_{i(i\pm1)}}\right) + \left(2\beta_{0i} + \beta_{pi}\cdot\frac{\partial \ln k_i}{\partial \ln p_i} + \beta_{ri}\cdot\frac{\partial \ln m_2}{\partial \ln r_2} + \right.$$

$$\left.\left. + \beta_{Q_{i(i\pm1)}}\cdot\frac{\partial \ln k_i}{\partial \ln Q_{(i\pm1)i}}\right)\frac{\beta_{0i}}{\beta_{0j}}\right] \right\},$$

(2.9)

where $A_i = d_i F_i \sigma_{0i} / \sum\limits_{i=1}^{3} d_i F_i \sigma_{0i}$  ($F_i = \sigma_{0i}/\sigma_i$); $k_i$ and $m_i$ are the

reduced thickness and mean grain size respectively; $\beta_{0i}/\beta_{0n}$ is equal $\beta_{01}/\beta_{02}$ (for the first layer); $\beta_{02}/\beta_{01}$ and $\beta_{03}/\beta_{02}$ (for the second layer) and $\beta_{03}/\beta_{02}$ (for the third layer).

If allow interlayer transitions 4 and 4" (see Fig. 2.2) then the right part is necessary to be supplemented by two summand in the brackets near the multiplicands $A_1$ and $A_3$.

It should be noted that this theoretical model can be easy carried over in case of any quantity of layers.

### 2.4 The macroscopic model

The double-layered film in the framework of macroscopic model can be presented as two ones in parallel connected resistors by analogy with the Dimmich model. Hence, equation for the total system resistivity is expressed by $\rho = \dfrac{\rho_1 \rho_2 (d_1 + d_2)}{\rho_1 d_2 + \rho_2 d_1}$. Logarithmic differentiation of this equation then gives

$$\beta = \beta_1 + \beta_2 + \frac{d_1 \alpha_1 + d_2 \alpha_2}{d_1 + d_2} - \frac{\beta_1 \rho_1 d_2 + \rho_1 d_2 \alpha_2 + \beta_2 \rho_2 d_1 + \rho_2 d_1 \alpha_1}{\rho_1 d_2 + \rho_2 d_1},$$

$$(2.10)$$

where $\alpha_i = \dfrac{1}{d_i} \dfrac{\delta d_1}{\delta T}$ is the coefficient of thermal expansion of the film thickness.

There are two limiting forms of equation (2.10):

1) when the thickness of first layer $d_1$ is constant, the thickness of second layer $d_2$ takes infinitive value. Equation (2.6) then becomes

$$\beta = \beta_1 + \beta_2 + \frac{d_2 \alpha_2}{d_2} - \frac{\beta_1 \rho_1 d_2 + \rho_1 d_2 \alpha_2}{\rho_1 d_2} = \beta_2 \, ;$$

2) when the thickness of second layer $d_2$ is constant, the thickness of first layer $d_1$ takes infinitive value. Equation (2.10) then becomes

$$\beta = \beta_1 + \beta_2 + \frac{d_1 \alpha_1}{d_1} - \frac{\beta_2 \rho_2 d_1 + \rho_2 d_1 \alpha_1}{\rho_2 d_1} = \beta_1 .$$

Hence, the values of $\beta_1$ and $\beta_2$ are the asymptotes for the TCR of the first and second layers respectively (Fig. 2.3).
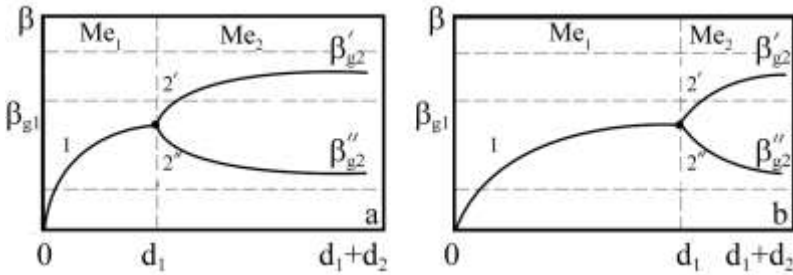


Figure 2.3 – The qualitative size dependences for double-layered films ($\beta_1(d_1)$ (1), $\beta_2(d_2)$ at $\beta_{g2} > \beta_{g1}$ (2) and $\beta_2(d_2)$ at $\beta_{g2} < \beta_{g1}$) in two limiting cases: $d_1 = $ const, $d_2 \to \infty$ (a), $d_2 = $ const, $d_1 \to \infty$ (b)

According to limiting forms of equation (2.10) the conclusions can be made as follows:

1) the value of the TCR of double-layered film increases with increasing the total film thickness assuming that $\beta_{g2} < \beta_{g1}$;

2) the value of the TCR of double-layered film decreases with increasing the total film thickness assuming that $\beta_{g2} > \beta_{g1}$.

The comparison between experimental data of the TCR with calculated values of the TCR using the macroscopic model is presented in Table 2.2. Experimental data better conform to calculated ones at low interdiffusion process.

In the case of multilayered film systems the general equation for the TCR in the framework of the macroscopic model can be rewritten in the following form:

$$\beta = \sum_{i=1}^{n} \beta_i + \frac{\sum_{i=1}^{n} d_i \alpha_i}{\sum_{i=1}^{n} d_i} - \frac{\sum_{i,k,m,\ldots=1}^{n} d_i \alpha_i \rho_k \rho_m \cdot \ldots}{\sum_{i,k,m,\ldots=1}^{n} d_i \rho_k \rho_m \cdot \ldots} -$$

$$- \frac{\sum_{i,k,m,\ldots=1}^{n} d_i \left( \beta_k + \beta_m + \ldots + \beta_n \right) \rho_k \rho_m \cdot \ldots d_i}{\sum_{i,k,m,\ldots=1}^{n} d_i \rho_k \rho_m \cdot \ldots}, \left( i \neq k \neq m \neq \ldots \right)$$

Table 2.2 – The experimental and calculated values of the TCR for double-layered film systems with the macroscopic model

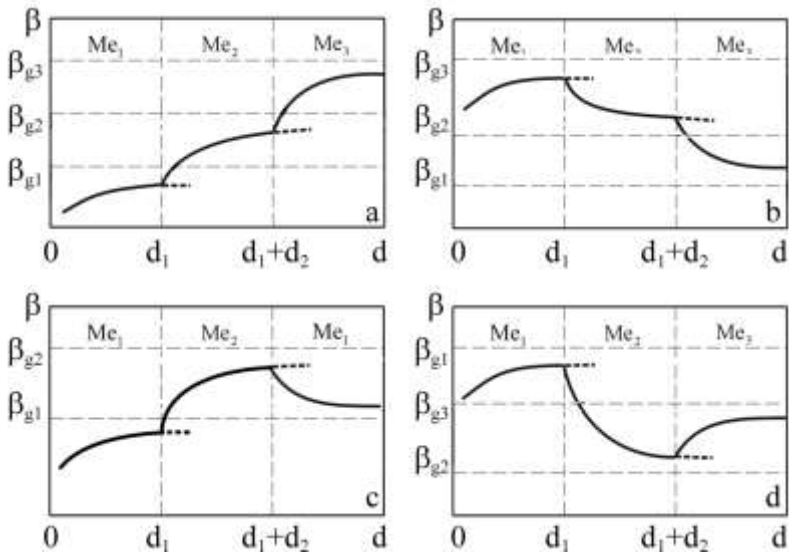| Film (d, nm) | $\beta_{\exp} \cdot 10^3$, $K^{-1}$ | $\beta_{\text{calc}} \cdot 10^3$, $K^{-1}$ |
|---|---|---|
| Cr(25)/Ni(10)/П | 1,41 | 1,22 |
| Cr(50)/Ni(55)/П | 1,69 | 2,88 |
| Cr(20)/Ni(20)/П | 1,19 | 2,61 |
| Cr(30)/Ni(40)/П | 1,64 | 3,02 |
| Sc(18)/Cu(48)/П | 2,10 | 2,30 |
| Sc(60)/Cu(30)/П | 1,76 | 2,17 |
| Sc(65)/Cu(43)/П | 1,90 | 2,18 |
| Sc(93)/Cu(38)/П | 1,69 | 2,17 |
| Cu(30)/Cr(30)/П | 1,64 | 1,94 |
| Cu(48)/Cr(15)/П | 2,22 | 2,26 |
| Cr(48)/Cu(55)/П | 2,58 | 2,71 |
| Ni(25)/Cr(75)/П | 1,08 | 1,79 |
| Ni(15)/Cr(25)/П | 1,44 | 1,64 |
| Ni(30)/Cr(45)/П | 1,61 | 2,32 |
| Ni(40)/Cr(60)/П | 1,85 | 2,58 |

Figure 2.4 – The qualitative size dependences for trilayered films: $\beta_{\infty 3} > \beta_{\infty 2} > \beta_{\infty 1}$ (a); $\beta_{\infty 3} < \beta_{\infty 2} < \beta_{\infty 1}$ (b) and the oscillated dependences (c, d)
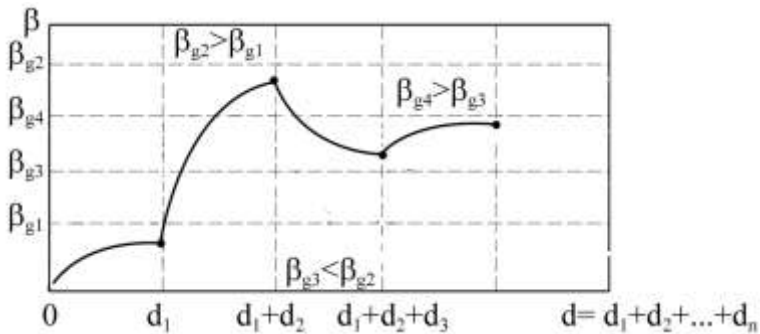


Figure 2.5 – The qualitative size dependences for multilayered film systems

The qualitative size dependences of the TCR for trilayered film and multilayered film system are presented at Fig. 2.4 and 2.5 respectively.

Thus, the size dependence of the TCR of multilayered film system has oscillated character. The value of the TCR both increasing and decreasing at the increase of the thickness, tends to the asymptotic value $\beta_g$. The materials of each layer can be chosen as the value of the TCR will only increase or only decrease.

## 2.5 Effects of thermal expansion and interdiffusion

In previous section the general expression for the electrical resistivity and the temperature coefficient of resistance has been proposed, including the effects of thermal expansion of the film thickness which appear at the interfaces both between the film and the substrate and between the layers. However, in most experiments related to thin metal films it is generally assumed that the thermal expansion coefficients of film thickness are negligible with respect to the bulk TCR, $\beta_0$.

Moreover one should not forget that thermal variations in the electrical parameters $p$, $R$, $r$ and $Q$ are not taken into account in calculations presented in Section 1 and 2.

The estimation method of thermal expansion significance values has been proposed by Protsenko I. Yu. et al.

For the reason that thermal expansion, in comparison with structural expansion, do not relax at the heat treatment, for estimation of thermal expansion significance value the following equations can be used:

$$S_T = \frac{E}{1 - \mu_f}\left(\alpha_f - \alpha_s\right)\Delta T, \ \Delta\varepsilon_T = \left(\alpha_f - \alpha_s\right)\Delta T, \qquad (2.7)$$

where $S_T$ is the thermal expansion, $\alpha_f$ and $\alpha_s$ are the coefficients of linear expansion of the film and substrate respectively, $E$ is Young's modulus, $\mu_f$ is Poisson's ratio of the film.

The pressure coefficient of resistance is relative change of the resistance at the pressure change: $\beta_p = \dfrac{1}{\rho}\dfrac{\partial \rho}{\partial p}$. The estimation of $(\rho/\rho)_{max}$ value was done by the extrapolation of the value of $\beta_p$ onto $p = S_T$. The calculations of $(\rho/\rho)_{max}$ at the maximum value of $\Delta\varepsilon$ and $S_T$ are presented in Table 2.3.

Table 2.3 − The calculation of the relative change of resistivity under expression

| Film | $E \cdot 10^{-10}$, H/m$^2$ | $\nu$ | $\alpha \cdot 10^6$, K$^{-1}$ | $\Delta\varepsilon_{max}$ $\cdot 10^3$ | $S_T \cdot 10^9$, H/m$^2$ | $\beta_p \cdot 10^{11}$, Pa$^{-1}$ | | $(\rho/\rho)_{max}$, % |
|------|------|------|------|------|------|------|------|------|
| | | | | | | $p = 0$ | $p = S_T$ | |
| Mo | 32.9 | 0.31 | 5.59 | 0.24 | 0.11 | 1.31 | 1.31 | 0.14 |
| Cr | 24.5 | 0.30 | 5.88 | 1.40 | 0.50 | 22.20 | 19.50 | 5.00 |
| Re | 76.1 | 0.26 | 6.70 | 0.70 | 1.00 | – | – | – |
| Ni | 20.2 | 0.30 | 14.98 | 4.00 | 1.10 | 1.77 | 1.81 | 2.00 |
| Ti | 10.4 | 0.36 | 7.70 | 10.80 | 0.20 | 1.19 | 1.18 | 0.24 |
| Sc | 6.6 | 0.30 | 11.40 | 25.60 | 0.26 | – | – | – |

One can make the general conclusion that the thermal expansion has no effect on the electrical resistivity and, as a result, on the TCR of the films.

The analysis of interdiffusion effects on the electrical resistivity and the TCR requires the following assumption:
− the diffusion of the impurity atoms occurs inside of the grains and at the grain boundaries, but only the second type of interdiffusion have an effect on the value of the scattering parameter $R$;
− at low concentration of the second-rate atoms the value of $R$ is changed proportionally to the concentration, i. e.

$R' = R + \gamma \cdot c$, where $R$ is the value of the scattering parameter at $c = 0$; $\gamma$ is the coefficient of proportionality which takes both positive and negative values.

On the basis of these assumptions, the estimation values of relative changes in $\Delta\rho/\rho_0$ and $\Delta\beta/\beta_0$ can be done in the framework such as the effective mean free path model (1.19) and (1.20″). The calculation procedure consists of the following steps:

1) calculation of the value of the specular parameter $R'$ at different values of $\gamma \cdot c$;

2) calculation of the value of the scattering parameter $\alpha$ at different values of $R'$: $\alpha = \lambda_0 L^{-1} R' (1 - R')^{-1}$;

3) calculation of the value of the function of grain boundary scattering $f(\alpha)$ (1.14);

4) calculation of the values of $\rho/\rho_0$ and $\beta/\beta_0$ in the framework of the effective mean free path model (1.19) and (1.20″);

5) calculation of the values $\Delta\rho/\rho_0$ and $\Delta\beta/\beta_0$, where $\Delta\rho = \rho(R') - \rho(R)$ and $\Delta\beta = \beta(R') - \beta(R)$.

The calculations showed that the change of the electrical resisitivity and the TCR amount to several percent.

## 2.6 References

1. Кузьменко А. І. Наукові праці Сумського державного педінституту. Серія : Фізика твердого тіла / А. І. Кузьменко, І. Ю. Проценко, А. М. Чорноус – Суми : СДПІ, 1993. – С. 29–34.
2. Однодворець Л. В. Електрофізичні та магніторезистивні властивості плівкових матеріалів в умовах фазоутворення / Л. В. Однодворець, С. І. Проценко, А. М. Чорноус. – Суми : Вид-во СумДУ, 2011. – 204 с.
3. Проценко І. Ю. Тонкі металеві плівки (технологія та властивості) : навчальний посібник / І. Ю. Проценко,

В. А. Саєнко. – Суми : Сумський державний університет, 2002. – 187 с.

4. Проценко С. І. Внесок температурних ефектів у термічний коефіцієнт опору багатошарових плівкових систем / С. І. Проценко, О. В. Синашенко, А. М. Чорноус // Металлофиз. Новейшие Технол. – 2005. – Т. 27, No. 12. – С. 1621–1633.

5. Проценко С. І. Структурно-фазовий стан, стабільність інтерфейсів та електрофізичні властивості двошарових плівкових систем (огляд) / С. І. Проценко, І. В. Чешко, Д. В. Великодний та ін. // Успехи Физ. Метал. – 2007. – Т. 8, No. 4. – С. 247–278.

6. Чорноус А. М. Розмірні ефекти в електрофізичних властивостях нанокристалічних плівкових систем в умовах взаємної дифузії та фазоутворення : автореф. дис. на здобуття наук. ступеня д-ра. фіз.-мат. наук : спец. 01.04.07 «Фізика твердого тіла» / А. М. Чорноус. – Суми, 2006. – 37 с.

7. Проценко И. Е. Температурная зависимость удельного сопротивления тонких пленок переходных 3-d металлов / И. Е. Проценко, М. Д. Смолин, А. В. Яременко и др. // УФЖ. –1988. – Т. 33, No. 6. – С. 875–880.

8. Borodin G. Electronic transport properties of double-layer metallic films / G. Borodin, F. Gallerani, A. Magnaterra // Appl. Phys. A. – 1990. – Vol. 50, No. 2. – P. 221–225.

9. Chornous A. Conductivity and temperature coefficient of resistance of multilayered polycrystalline films / A. Chornous, L. Dekhtyaruk, M. Marszalek, I. Protsenko // Cryst. Res. Technol. – 2006. – Vol. 41, No. 4. – P. 388–399.

10. Dekhtyaruk L. V. Conductivity and the temperature coefficient of resistance of two-layer polycrystalline films / L. V. Dekhtyaruk, S. I. Protsenko, A. M. Chornous et al. // Ukr. J. Phys. – 2004. – Vol. 49, No 6. – P. 587–597.

11. Dimmich R. Electrical conductance and TCR of double-layer films / R. Dimmich // Thin Solid Films. – 1988. – Vol. 158, No. 1. – P. 13–24.

12. Dimmich R. The electrical conductance of continuous thin metallic double-layer films / R. Dimmich, F. Warkusz // Thin Solid Films. – 1983. – Vol. 109. – P. 103.

13. Protsenko I. Size effect and processes of interdiffusion in multilayer films / I. Protsenko, S. Petrenko, L. Odnodvoretz et al. // Cryst. Res. Technol. – 1995. – Vol. 30, No. 8. – P. 1077–1081.

14. Tellier C. R. Size effects in thin films / C. R. Tellier, A. J. Tosser. – New York : Elsevier, 1982. – 310 p.

## SECTION 3
## Strain effect in thin films

### 3.1 Introduction

In previous sections the features of electrical resistivity and temperature coefficient of resistance of thin films and double-layered films have been studied from a theoretical point of view. The predicted results were compared with experimental data. In this section the variations in film resistivity with stress are examined first. The method of strain coefficient measurement is discussed and, finally some theoretical models of size effect in strain coefficient of thin film and double-layered film are then summarized.

### 3.2 The concept of size effect in strain

It is known from the previous sections that electro-physical properties of thin films usually differ from bulk materials. It is explained by size effects and features of crystal structure. Besides, electrical properties are strongly affected by temperature effects and defect concentration. It is important to note that mechanical stress is affected on resistance too. The variations in film resistivity with strain or compression are tensoresistive effect. From physical point of view tensoresistive effect is caused by the processes which appear inside of crystal at microscopical level (increasing or decreasing latticed parameter) and at the interface of the film or at the grain boundaries at microscopical and macroscopical levels (change of different type defects concentration, extension or decrease of the crystallite size, emergence of the localized energy level, change of parameters $p$, $r$, etc.).

The mechanical properties of thin films can be studied by introducing the mechanical parameters which are usually

defined for bulk materials, i. e. Young's modulus and Poisson's ratio.

Young's modulus, $E$, of an isotropic bulk material is the reciprocal ratio of the differential strains in the length, width and thickness directions $d/dl$, $d/da$, $d/dd$ respectively, to the stress applied in the corresponding direction $dS_l$, $dS_a$, $dS_d$ respectively, i. e.

$$E = \frac{d}{dl} \cdot \frac{1}{S_l} = \frac{d}{da} \cdot \frac{1}{S_a} = \frac{d}{dd} \cdot \frac{1}{S_d}. \qquad (3.1)$$

The Poisson's ratio of the film $\mu_f$ of an isotropic bulk material expresses the differential strain in the direction perpendicular to that of the applied stress. For instance, the strain in the $d$-direction, $d/dd$, is related to the longitudinal strain $d/dl$ due to a stress applied in the $l$-direction by the equation (Fig. 3.1)

$$\frac{d}{dd} = -\mu_f \frac{d}{dl} \implies \mu_f = -\frac{d/dd}{d/dl}. \qquad (3.2)$$

In case of thin metal films a preferred orientation often exists and it could be necessary to introduce several Poisson's ratios for an accurate description of the phenomena. In most cases, the preferred direction for nucleation is perpendicular to the surface of the substrate, so that two mechanical parameters can be useful: the Poisson's ratios $\mu_{f1}$, $\mu_{f2}$; when a stress is applied in the $l$-direction, the strains induced in $a$- and $d$-directions are then given by

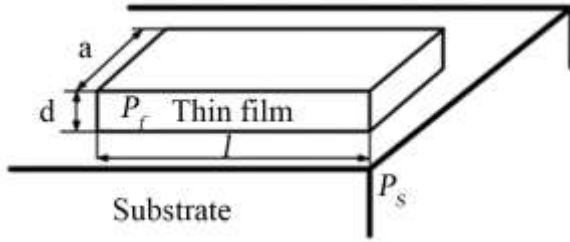$$\mu_{f1} = -\frac{d/dd}{d/dl}, \quad \mu_{f2} = -\frac{d/da}{d/dl}.$$

Figure 3.1 – Geometry of strain sensitive device

If the substrate has no mechanical action, i. e. one may consider that the film is not attached to a substrate.

In case of supported films, a mechanical stress applied to the film substrate induces strains in the film; it is generally assumed that the strains applied to an attached film in the $l$- and $w$-directions are identical to the strains induced in the substrate by stress applied to the substrate, whereas the strain in the $d$-direction is determined by the mechanical properties of the film subjected to strains in both $l$- and $a$-directions. For instance, a longitudinal mechanical stress applied to the film substrate leads to: a longitudinal strain $dl_s/l_s$ in substrate length $l_s$; to a transverse strain $da_s/a_s$ in substrate width $a_s$, the strains obey the relation $\mu_s = -\dfrac{da_s/a_s}{dl_s/l_s}$, where $\mu_s$ is the Poisson's ratio of the substrate.

The strains in film length and width are then $\dfrac{dl}{l} = \dfrac{dl_s}{l_s}$

and $\dfrac{da}{a} = -\mu_f \dfrac{da_s}{a_s}$.

The strain in film thickness is due to the superimposed effects of the stresses acting in the $l$- and $a$-directions; these stresses are not directly measurable and we know only that the resulting effects of both stresses are the strains $dl/l$ and $da/a$.

Therefore one should bear in mind that the effect of the longitudinal (transverse) stress is a fictive longitudinal (transverse) strain $\varepsilon_l$ ($\varepsilon_t$) which differs from $dl/l$ ($da/a$), i. e.

$$\varepsilon_l = \frac{dl}{l} \left( \varepsilon_t = \frac{da}{a} \right).$$

The quantitative characteristic of tensoresistive effect is strain coefficient ($\gamma$). The general definitions of the longitudinal ($\gamma_l$) and transverse ($\gamma_t$) strain coefficients of resistance are

$$\gamma_l = \frac{dR/R}{dl/l} = \frac{dR/R}{\varepsilon_l}, \ \gamma_t = \frac{dR/R}{dw/w} = \frac{dR/R}{\varepsilon_t}. \qquad (3.3)$$

Notice that the current direction is parallel to the deformation direction at the longitudinal stress and the current direction is perpendicular to the deformation direction at the transverse stress. This is the main reason of different values $\gamma_l$ and $\gamma_t$, as a rule $\gamma_l > \gamma_t$.

### 3.3 The experimental method of strain coefficients measurement

On the basis of equation (3.1.) we can confirm that

$$\frac{dR}{R} = \gamma_l \varepsilon_l, \ \frac{dR}{R} = \gamma_t \varepsilon_t.$$

Hence, the value of strain coefficients $\gamma_l$ or $\gamma_t$ may be accurately calculated from the slope of the dependence $dR/R$ in comparison with strain. It is necessary to note that strain dependence has linear law at the definite curve piece only; therefore the linear section of the strain dependence may be

considered at the determination of strain coefficients. In practice, it is done to calculate integral ($\gamma_{int}$) and differential ($\gamma_{dif}$) strain coefficients. The calculation of integral and differential strain coefficients is carried out by equations:

$$(\gamma_l)_{int} = \frac{1}{R(0)}\frac{\Delta R}{\Delta\varepsilon_l}, \quad (\gamma_l)_{int} = \frac{1}{R_i}\frac{dR_i}{d\varepsilon_{li}}, \qquad (3.5)$$

where $R(0)$ is resistance at zero longitudinal deformation; $R_i$ and $dR_i$ are resistance of the thin film sample at the beginning of the strain interval $\Delta\varepsilon_{li}$ and their change at the increase of longitudinal strain respectively.

The problem of the strain value determination is more difficult in this case. Consider two types of strain: expansion and bending (Fig. 3.2).

In the first case $\varepsilon_l$ is equal to $\varepsilon_t$. According to the Figure 3.2 b geometry can find the equation for this strain:

$$\varepsilon_l = \frac{AB - A_0 B_0}{A_0 B_0} = \frac{R - R_0}{R_0} = \frac{D/2}{R_0},$$

$$(R_0 - h)^2 + l_n^2 = R_0^2 \Rightarrow R_0 = \frac{h^2 + l_{in}^2}{2h},$$

$$\varepsilon_l = \frac{D \cdot h}{l_{in}^2}, \qquad (3.6)$$

where $l_{in}$ is the initial value of the samples length.

In the second case, it is necessary to separately calculate strain as $\varepsilon_l = \dfrac{\Delta l}{l_{in}}$ and $\varepsilon_t = \dfrac{\Delta a}{a_{in}}$, where $a_{in}$ is the initial value of the samples width.

The example of dependences $\Delta R/R$, $R$ and $\gamma_{li}$ in comparison with $\varepsilon_l$ for Pt(20)/S thin film is presented in Fig. 3.3.
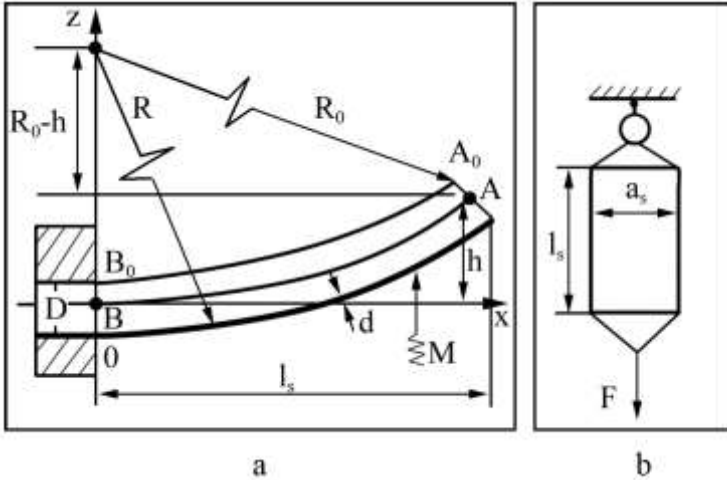
Figure 3.2 – The method of strain value determination at bending (a) and expansion (b): $A_0B_0$ is neutral surface track, $R$ is neutral surface radius, $Ox$ is baseline, $h$ is maximal flexure, $D$ and $d$ are the thicknesses of the substrate and the film respectively, $l$ and $w$ are the initial length and width of the film, $M$ is microscrew, $F$ is force
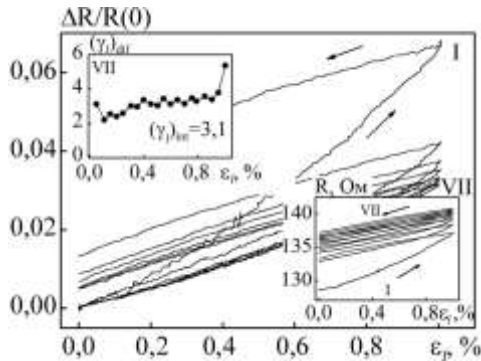


Figure 3.3 – Dependences $\Delta R/R(0)$, $R$ and $(\gamma_l)_{dif}$ versus $\varepsilon_l$ for Pt(20)/S thin film at $\Delta\varepsilon_{l1} = 0$–1 %. I, VII are numbers of deformation cycles "load – unload"

### 3.4 Theoretical expression of strain coefficients of thin films

The analysis of experimental results for thin film strain coefficients showed that the value of $\gamma$ depends on its thickness as a result of the size effect.

In this item the theoretical models for strain coefficients of monocrystalline and polycrystalline thin films will be described.

### 3.4.1 Fuchs and Sondheimer model

In the framework of Fuchs and Sondheimer conduction model the calculations of the strain coefficients begin from the equation for resistance

$$R = \rho \frac{l}{a \cdot d}$$

or

$$lnR = ln\rho + lnl - lna - lnd.$$

After differentiation:

$$\frac{dR}{R} = \frac{\partial \rho}{\rho} + \frac{\partial l}{l} - \frac{\partial a}{a} - \frac{\partial d}{d}.$$

On the basis of definition of the longitudinal and transverse strain coefficients the equations for $\gamma_l$ and $\gamma_t$ can be written in the form

$$\gamma_l = \frac{dR/R}{dl/l} = \frac{\partial \rho / \rho}{\partial l / l} + (1 + 2\mu_f), \qquad (3.7)$$

$$\gamma_l = \frac{dR/R}{da/a} = \frac{\partial\rho/\rho}{\partial a/a} - 1, \qquad (3.8)$$

since $\dfrac{\partial a/a}{\partial l/l} = -\mu_{\mathrm{f}}$.

For comparison of equations (3.7) and (3.8) with analogous ones for bulk materials (thick film samples) it is necessary to be out of the equation $\rho \sim (n\lambda_0)^{-1}$, where $n$ is the concentration of electrons. Then, taking into account that resistance for bulk materials can be written as $R_0 = \rho_0 \dfrac{l_0}{w_0 d_0}$, we receive

$$\gamma_{0l} = -\frac{dn/n}{dl/l_0} - \frac{d\lambda_0/\lambda_0}{\partial l/l_0} + (1 + 2\mu_f)$$

or

$$\gamma_{0l} \cong \eta_{0l} + 2(1 + 2\mu), \qquad (3.9)$$

where $\eta_{0l}$ is the deformation coefficient of the electron mean free path in the bulk material.

For thin film with thickness in the range from 20 to 600 nm the FS model gives

$$\gamma_l = \gamma_{l0} - \left(\frac{Y}{F}\right) \cdot \left(\eta_{0l} - \mu_f\right), \qquad (3.10)$$

where $(Y/F)$ is relations of the famous function, $\gamma_{l0}$ is the longitudinal strain coefficient of the bulk monocrystal.

From equations (3.10) it follows that $\gamma_l > \gamma_{l0}$ at $\eta_{0l} < \mu_{\mathrm{f}}$ and vice versa. The similar result was received for the transverse strain coefficient $\gamma_t$.

65

### 3.4.2 Effective mean free path model of Tellier, Tosser and Pichard

The equation for conductivity in the framework of Mayadas – Shatzkes model for size effect in electrical resistivity can be used for calculation of strain coefficient

$$\sigma = \sigma_0 [f(\alpha) - A(k, p, \alpha)], \qquad (3.11)$$

where $\sigma_0$ is the bulk conductivity; $f(\alpha)$ is the function of electrons grain boundary scattering described in detail in Section 1;

$$A(k, p, \alpha) = \frac{6}{\pi k}(1-p)\int_0^{2\pi} d\Phi \int_1^8 dt \, \frac{\cos^2 \Phi}{H^2(t, \Phi)}\left(\frac{1}{t^3} - \frac{1}{t^5}\right) \times$$

$$\times \frac{1 - \exp[-ktH(t, \Phi)]}{1 - p} \exp[-ktH(t, \Phi)];$$

$$H(t, \Phi) = 1 + \frac{\alpha}{\cos \Phi \sqrt{1 - t^2}}, \quad t = \cos^{-1}\Theta,$$

where $\Theta$ is angle between velocity vector $\upsilon$ and direction $z$.

The differentiation of equation (3.11) by strain allows to give the equation for strain coefficient

$$\gamma_l = \gamma_{0l}^\rho + [f(\alpha) - A(k, p, \alpha)]^{-1} \cdot \left\{ (\eta_{\lambda l0} + \beta)X - \left(1 + \mu_f \frac{1 - \mu_s}{1 - \mu_f}\right)Y' \right\} +$$

$$+ 1 + \mu_s + \mu_f \frac{1 - \mu_s}{1 - \mu_f}, \qquad (3.12)$$

where $X$ and $Y'$ are known functions.

### 3.4.3 Linearized model of Tellier, Tosser and Pichard

The model of FS is closely applied for thin film in the case when $\gamma < \gamma_0$ but not in the case when $\gamma > \gamma_0$. However, there are many experimental data for high-melting thin films or thin film with relatively high melting temperature which are characterized by regularity $\gamma > \gamma_0$ (Fig. 3.3).
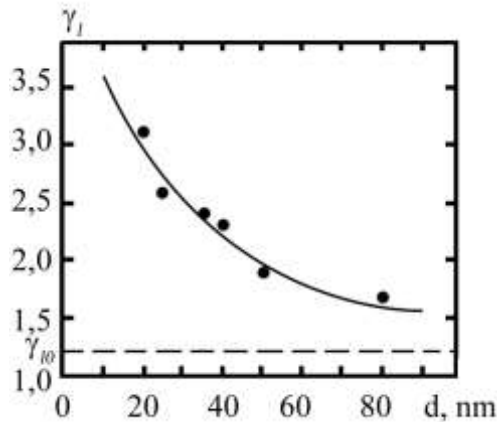


Figure 3.3 – The experimental size dependence of the Pt thin films strain coefficient ($\gamma_{l0}$ is the asymptote of the exponential dependence)

Therefore K. Tellier, A. Tosser and K. Pichard on the basis of the Mayadas – Shatzkes model and effective mean free path model received the equation for strain coefficients in case when $\gamma > \gamma_0$. In the first approximation the equations for $\gamma_l$ and $\gamma_t$ are

$$\gamma_l = (\eta_l + 1)f(\alpha)d - (1 - p)\lambda_0[(\eta_l + 1)f(\alpha)H(\alpha) - (1 - \mu')U(\alpha)],$$

(3.13)

where $H(\alpha)$ and $U(\alpha)$ are the known and tabulated functions; $\mu' = \dfrac{\mu_s(1-\mu_s)}{(1-\mu_f)}$ is reduced Poisson's ratio for thin film.

The linearized equation (3.13) allows calculating parameters $\eta_l$, $\lambda_0$, $p$. For this purpose, it is necessary to plot experimental data in the form $\gamma_l \cdot d$ in comparison with $d$. This graph is a straight line with a slope $(\eta_l + 1)f(\alpha)$ and an ordinate interception $(1-p)\lambda_0[(\eta_l+1)f(\alpha)H(\alpha)-(1-\mu')U(\alpha)]$.

### 3.4.4 Three-dimensional model of Tellier, Tosser and Pichard

The linearized model can be used in case if $L > d$ only. But K. Tellier, A. Tosser and K. Pichard in the frame of three-dimensional model for electrical conductivity have proposed more general three-dimensional model for strain. For the theoretical characterization of independent electron scattering at the grain boundaries and external surfaces of the thin film the following parameters have been used:

$$\nu = L\lambda_0^{-1}\left(\ln\frac{1}{r}\right)^{-1}, \qquad \mu = d\lambda_0^{-1}\left(\ln\frac{1}{p}\right)^{-1}.$$

In addition, three-dimensional model assumes that crystallites have arbitrary shape, so in general case $L_x \neq L_y \neq L_z$.

The equation for longitudinal strain coefficient has been written in the form

$$\gamma_l = (\eta_l + 1) - \eta_l \frac{F'(\nu_x)+G'(\nu_y)+G'(\alpha')}{M(\nu_x,\nu_y,\alpha')}$$
$$+ \frac{\mu_s G'(\nu_y)\_F'(\nu_x)+\mu'G'(\alpha')}{M(\nu_x,\nu_y,\alpha')}, \tag{3.14}$$

$$M(v_x, v_y, \alpha') = \frac{\rho}{\rho_0} = F(v_x)^{-1} + G(v_y)^{-1} + G(\alpha')^{-1} - 2,$$

$$F'(v_x) = v_x \cdot f(v_x) \cdot F(v_x)^{-2}, \ G'(v_y) = v_y \cdot g(v_y) \cdot G(v_y)^{-2},$$

$$G'(\alpha) = \alpha' \cdot g(\alpha') \cdot G'(\alpha')^{-2}, \ (\alpha)^{-1} = \mu^{-1} + v_z^{-1},$$

where $F(v_x)$, $G(v_y)$, $G'(\alpha')$, their derivatives $f(v_x) = \dfrac{dF}{dv_x}$, $g(v_y) = \dfrac{dG}{dv_y}$, $g(\alpha') = \dfrac{dG}{d\alpha'}$ are known functions.

The value of longitudinal strain coefficient can be received if the experimental or calculated data are used. The similar equations can be written for the transverse strain coefficient. The approbation of the three-dimensional model of experimental data for Cr thin films allows to ascertain that the equation (3.14) complies with experimental data at complementary assumption about size dependence of coefficient $\eta_l$: $\eta_l = 9,70$ ($d = 30$ nm); 7,60 (45 nm); 1,73 (65 nm); 1,00 (90 nm). Note that the idea of size dependence of $\eta_l$ is unexceptionable because quantity of parameters depends on film thickness. Specifically, the mean free path in film $\lambda_g = \lambda \cdot f(\alpha)$ depends on thickness.

### 3.5 Experimental data for thin films strain coefficients

Measurements of the longitudinal and transverse strain coefficients of metal thin films are widely presented in the literature. It allows to receive experimental size dependences of the strain coefficient for different thin film materials (Fig. 3.4).

On the basis of literature data the regularity of size effect in strain can be formulated:

1) the value of strain coefficient in the thin monocrystalline films can be smaller or bigger than the value for samples in bulk state;

2) the size effect of strain coefficient in the polycrystalline thin films has the features as follows:
– the value of $\gamma_l$ is almost always bigger than the value of $\gamma_t$. It is explained by features of crystal lattice inner potential changes in deformation;
– the value of strain coefficients can increase or decrease at the thickness (crystallite size) increasing subject to surface-grain boundary scattering relation;
3) the value of $\gamma_l$ and $\gamma_t$ strongly depends on the number of deformation cycles as a result of residual deformation;
4) stain coefficients do not depend on substrate materials;
5) the value of $\gamma_l$ and $\gamma_t$ changes as linear law subjects to measurement temperatures;
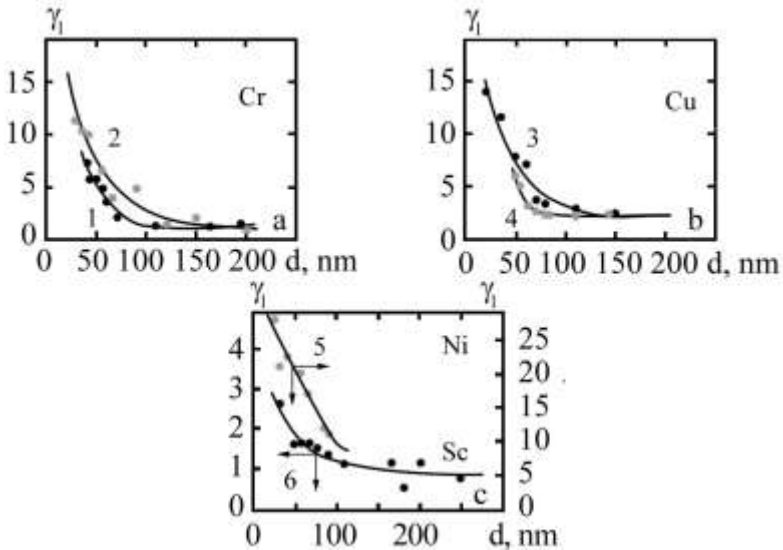


Figure 3.4 – Size dependences of longitudinal strain coefficient for thin films: Cr (1, 2); Cu (3, 4); Sc (5); Ni (6). 1, 4, 5 are teflon and Ni foil substrates; 2, 3, 6 are glass-fibre laminate substrates

6) the value of $\gamma_l$ and $\gamma_t$ monotonously decreases during samples aging;

7) the value of $\gamma_l$ and $\gamma_t$ at bending deformation is significantly bigger than at expansion deformation under similar conditions.

These behaviors are typical for transition of *d*-metal thin films and not always appear for low-melting metal and discontinuous (island) films.

### 3.6 Size effects in strain of double-layered films

Tensosensitivity of thin metal films is significantly lower in comparison with semiconductor thin films. One of the method of it increasing is using double or multilayered thin film systems. The main difference of double-layered thin film systems from single-layered is that new mechanism of the conduction electron scattering at interfaces appears.

### 3.6.1 The microscopic model

For developing the double-layered model it is necessary to make assumption that double-layered film can be presented as parallel connection of two thin films with resistance $R_1$ and $R_2$:

$$\frac{1}{R} = \frac{1}{R_1} + \frac{1}{R_2} = \frac{1}{\rho_1 l_1 /(a_1 d_1)} + \frac{1}{\rho_2 l_2 /(a_2 d_2)} = \frac{a}{l}(\sigma_1 d_1 + \sigma_2 d_2),$$

where $l_1 = l_2 = l$, $a_1 = a_2 = a$, $\sigma$ is conductivity.

If the function of Sondheimer denotes that $F = \sigma/\sigma_0$, then previous equations can be rewritten as

$$\frac{1}{R} = \frac{a}{l}\left(\sigma_{01} F_1\left(d_1, \lambda_{01}, p_1^*, r_1\right) d_1 + \sigma_{02} F_2\left(d_2, \lambda_{02}, p_2^*, r_2\right) d_2\right), \quad (3.15)$$

71

where $p_1^* = \dfrac{p_{10} + p_{12}}{2}$ and $p_2^* = \dfrac{p_{20} + p_{12}}{2}$ are effective specularity parameters, $p_{10}$, $p_{12}$, $p_{20}$ are specularity parameters at the interfaces of first layer-substrate, first layer-second layer, second layer-vacuum respectively.

Equations for $\gamma_l$ and $\gamma_t$ can be received at assumption that

$$\frac{\Delta l}{l} \cong \varepsilon_l, \quad \frac{\Delta a}{a} \cong \varepsilon_t, \quad -\frac{\Delta d / d}{\Delta l / l} \cong \mu_f \cdot \frac{1 - \mu_s}{\mu_f} \cong \mu'.$$

For this purpose it is necessary to take logarithmic differential from the left and right part of equation (3.15):

$$\frac{dR}{R_{in}} = -\left( \frac{dd_1}{d_1} + \frac{d\sigma_{01}}{\sigma_{01}} + \frac{dF_1}{F_1} \right) \cdot \left( \frac{d_1 d\sigma_{01} dF_1}{d_1 d\sigma_{01} dF_1 + d_2 d\sigma_{02} dF_2} \right) -$$

$$-\left( \frac{dd_2}{d_2} + \frac{d\sigma_{02}}{\sigma_{02}} + \frac{dF_2}{F_2} \right) \cdot \left( \frac{d_2 d\sigma_{02} dF_2}{d_1 d\sigma_{01} dF_1 + d_2 d\sigma_{02} dF_2} \right) - \left( \frac{da}{a_{in}} - \frac{dl}{l_{in}} \right).$$

$$(3.16)$$

Considering that $\gamma_l = \dfrac{dR / R_{in}}{dl / l_{in}}$, $\gamma_t = \dfrac{dR / R_{in}}{da / a_{in}}$ and at addition that $p^*$ and $r$ do not depend on temperature, the equation (3.16) can be rewritten in the form

$$\gamma_l = \frac{dR / R_{in}}{dl / l_{in}} = A_1 \cdot \left( \mu_1' + 1 + \eta_{0l1} - \frac{d \ln F_1}{d \ln l} \right) +$$

$$+ A_2 \left( \mu_2' + 1 + \eta_{0l2} - \frac{d \ln F_2}{d \ln l} \right) + 1 + \mu_s$$

or

$$\gamma_t = \frac{dR / R_{in}}{da / a_{in}} = A_1 \cdot \left( \mu_1' + 1 + \eta_{01t} - \frac{d \ln F_1}{d \ln a} \right) +$$
$$+ A_2 \cdot \left( \mu_2' + 1 + \eta_{0t2} - \frac{d \ln F_2}{d \ln a} \right) - 1 - \mu_s,$$

where it is taken into account that $-\dfrac{d \ln \sigma_0}{d \ln l} = 1 + \eta_{0l}$,

$-\dfrac{d \ln \sigma_0}{d \ln a} = 1 + \eta_{0t}$ and coefficients $A_i$ are determined by analogy with equation (2.5).

Whereas $\dfrac{d \ln k_1}{d \ln l} = \dfrac{d}{d \ln l} \left( \ln d - \ln \lambda_0 \right) = -\mu_1' + \eta_{\lambda_0 l_1}$ then

$$\frac{d \ln F_i}{d \ln l} = \frac{d \ln F_i}{d \ln k_i} \left( \eta_{0li} - \mu_l' \right) + \frac{d \ln F_i}{d \ln k_i} \left( \eta_{0li} - \mu_k' \right) \frac{d \ln k_i}{d \ln k_k},$$

$$\frac{d \ln F_i}{d \ln a} = \frac{d \ln F_i}{d \ln k_i} \left( \eta_{0ti} - \mu_l' \right) + \frac{d \ln F_i}{d \ln k_i} \left( \eta_{0ti} - \mu_k' \right) \frac{d \ln k_i}{d \ln k_k} \qquad \text{and}$$

$$\frac{d \ln F_i}{d \ln k_i} = 1 - \frac{\beta_i}{\beta_{0i}}, \quad \frac{d \ln k_i}{d \ln k_k} = \frac{\beta_{0i}}{\beta_{0k}}, \quad (k_i = d_i / \lambda_{0i}, \ i, \ k = 1, 2; \ i \neq k),$$

the equation for strain coefficients take form

$$\gamma_l = A_1 \cdot \left[ \left( \gamma_{0 1 l} + \mu_1' \right) + \left( 1 - \frac{\beta_1}{\beta_{01}} \right) \left( -\gamma_{0 1 l} + \mu_1' \right) + \left( -\gamma_{0 1 l} + \mu_2' \right) \frac{\beta_{01}}{\beta_{02}} \right] +$$
$$+ A_2 \cdot \left[ \left( \gamma_{0 2 l} + \mu_2' \right) + \left( 1 - \frac{\beta_2}{\beta_{02}} \right) \left( -\gamma_{0 2 l} + \mu_2' \right) + \left( -\gamma_{0 2 l} + \mu_2' \right) \frac{\beta_{02}}{\beta_{01}} \right] +$$
$$+ 1 + \mu_s;$$

$$(3.17)$$

$$\gamma_t = A_1 \cdot \left[ \gamma_{0 1 t} - \left( 1 - \frac{\beta_1}{\beta_{02}} \right) \cdot \left( \gamma_{0 2 t} - 1 - \mu_2' \right) \frac{\beta_{01}}{\beta_{02}} \right] +$$

$$+A_2 \cdot \left[ \gamma_{02t} - \left( 1 - \frac{\beta_2}{\beta_{02}} \right) \cdot \left( \gamma_{01t} - 1 - \mu_1' \right) \frac{\beta_{02}}{\beta_{01}} \right] - 1 - \mu_s, \qquad (3.18)$$

where it is taken into account that $\gamma_{0li}^{\rho} = 1 + \eta_{0l}$ and $\gamma_{0ti}^{\rho} = 1 + \eta_{0t}$.

Note that one of the reason of deviation between calculated (3.17), (3.18) and experimental data is assumption that coefficients $p^*$ and $r$ do not depend on film strain. In this connection, Protsenko I. Yu. et al. proposed theoretical model which takes into account strain dependence of scattering parameters.

The double-layered film in the framework of this model can be presented as three ones in parallel connected resistors, so equation for the total system resistance may be written as

$$\frac{1}{R} = \frac{a}{l} \left[ \sigma_{01} F_1 \left( d_1, \lambda_{01}, p_1^*, r_1 \right) d_1 + \sigma_{02} F_2 \left( d_2, \lambda_{02}, p_2^*, r_2 \right) d_2 \right], \quad (3.19)$$

where $p_i^*$ is effective specularity parameter ( $p_1^* = \dfrac{p_{1n} + p_{12}}{2}$, $p_2^* = \dfrac{p_{20} + p_{12}}{2}$ ; $p_{1n}$, $p_{12}$ and $p_{20}$ are specularity parameters at the boundary film/substrate, at the interface and at the boundary film/vacuum respectively.

Logarithmic differentiation of this equation gives

$$\frac{dR}{R} = -\left( d \ln d_1 + d \ln \sigma_{01} + d \ln F_1 \right) A_1 - \left( d \ln d_2 + d \ln \sigma_{02} + d \ln F_2 \right) A_2 - $$
$$- \left( \ln a - d \ln l \right),$$

where $A_i = \dfrac{F_i \sigma_{0i} d_i}{\displaystyle\sum_{i=1}^{2} F_i \sigma_{0i} d_i}$ (at calculation it is more logical to use

the value $\sigma_{gi} \equiv \sigma_{0i} \cdot f(\alpha)$, where f(α) and $\sigma_0$ are the function of grain boundary scattering and conductance of bulk monocrystal respectively); $\mu_{f_1}' = -\dfrac{d \ln d_i}{d \ln l} \cong \mu_{f_1}$ is the Poisson's coefficient.

In this theoretical model it has been considered that function $F_i$ depends on both the reduced thickness $k = \dfrac{d}{\lambda_0}$, the effective specularity parameter p*, r and the reduced mean grain size $m = \dfrac{L}{\lambda_0}$ and the parameter of interface scattering $Q$. The derivative of the function $F_i$ at $i = 1$ can be written as

$$\frac{d \ln F_1\left(k_1, m_1, p_1^*, r_1, Q\right)}{d \ln l} = \left(\frac{d \ln F}{d \ln k_1} \frac{d \ln k_1}{d \ln l} + \frac{d \ln F_1}{d \ln m_1} \frac{d \ln m_1}{d \ln l}\right) +$$

$$+\left(\frac{d \ln F}{d \ln k_1} \frac{d \ln k_1}{d \ln k_{\backslash 2}} \frac{d \ln k_{\backslash 2}}{d \ln l} + \frac{d \ln F_1}{d \ln m_1} \frac{d \ln m_1}{d \ln m_2} \frac{d \ln m_2}{d \ln l}\right) +$$

$$+\left(\frac{d \ln F}{d \ln k_1} \frac{d \ln k_1}{d \ln p_1^*} \frac{d \ln p_1^*}{d \ln l} + \frac{d \ln F_1}{d \ln m_1} \frac{d \ln k_1}{d \ln Q} \frac{d \ln Q}{d \ln l}\right) +$$

$$+\left(\frac{d \ln F}{d \ln k_1} \frac{d \ln k_1}{d \ln k_{\backslash 2}} \frac{d \ln k_2}{d \ln p_2^*} \frac{d \ln p_2^*}{d \ln l} + \frac{d \ln F}{d \ln k_1} \frac{d \ln k_1}{d \ln k_{\backslash 2}} \frac{d \ln k_2}{d \ln Q} \frac{d \ln Q}{d \ln l}\right).$$

(3.20)

Since $\dfrac{d \ln F_i}{d \ln l} = \dfrac{d \ln F_i}{d \ln k_i}\left(\eta_{\lambda_{0i}l} - \mu_i'\right) + \dfrac{d \ln F_1}{d \ln k_i}\left(\eta_{\lambda_{0i}l} - \mu_k'\right) \times$

$\times \dfrac{d \ln k_i}{d \ln k_k}$, then after substituting in the previous equation, taking into account that $\dfrac{d \ln F_i}{d \ln k_i} = 1 - \dfrac{\beta_i}{\beta_{0i}}$, $\dfrac{d \ln k_i}{d \ln k_k} = \dfrac{\beta_{0i}}{\beta_{0k}}$

75

($i$, $k = 1$, 2 and $i \neq k$), the equation for the strain coefficient of double-layered film is

$$\gamma_l = A_1\left\{\left(\gamma_{0l1}^\rho + \mu_1'\right) - \left(1 - \frac{\beta_1}{\beta_{01}}\right)\left[\left(2\gamma_{0l1}^\rho - 1 - \mu_1' - \eta_{p^*l1}\frac{d\ln k_1}{d\ln p_1^*} - \right.\right.\right.$$

$$\left.- \eta_{Ql1}\frac{d\ln k_1}{d\ln Q_1} - \eta_{rl1}\frac{d\ln m_1}{d\ln r_1} + \left(2\gamma_{0l2}^\rho - 1 - \mu_2' - \eta_{p^*l2}\frac{d\ln k_2}{d\ln p_2^*} - \right.\right.$$

$$\left.\left.\left.- \eta_{Ql2}\frac{d\ln k_2}{d\ln Q_2} - \eta_{rl1}\frac{d\ln m_2}{d\ln r_2}\right)\frac{\beta_{01}}{\beta_{02}}\right]\right\} + A_2\left\{\left(\gamma_{0l2}^\rho + \mu_1'\right) - \left(1 - \frac{\beta_2}{\beta_{02}}\right)\cdot\right.$$

$$\cdot\left[\left(2\gamma_{0l2}^\rho - 1 - \mu_2' - \eta_{p^*l2}\frac{d\ln k_2}{d\ln p_2^*} - \eta_{Ql2}\frac{d\ln k_2}{d\ln Q_2} - \eta_{rl1}\frac{d\ln m_2}{d\ln r_2}\right) + \right.$$

$$\left.\left.+ \left(2\gamma_{0l1}^\rho - 1 - \mu_1' - \eta_{p^*l1}\frac{d\ln k_1}{d\ln p_1^*} - \eta_{Ql1}\frac{d\ln k_1}{d\ln Q_1} - \eta_{rl1}\frac{d\ln m_1}{d\ln r_1}\right)\frac{\beta_{02}}{\beta_{01}}\right]\right\} +$$

$$+ 1 + \mu_s,$$

(3.21)

where $\eta_Q = -\dfrac{1}{Q}\cdot\dfrac{dQ}{d\varepsilon_l}$ $(Q = Q_{12} = Q_{21})$; $\eta_r = -\dfrac{1}{r}\cdot\dfrac{dr}{d\varepsilon_l}$ and

$\eta_p = -\dfrac{1}{Q}\cdot\dfrac{dQ}{d\varepsilon_l}$ are strain coefficients of scattering parameter.

Derivatives can be approximately represented then as

$$\frac{d\ln k}{d\ln p^*} \cong \frac{\Delta\ln k}{\Delta\ln p^*} = \left(\ln\frac{\lambda_0(0)}{\lambda_0(\varepsilon_l)}\right)\bigg/\left(\ln\frac{p^*(\varepsilon_l)}{p^*(0)}\right),$$

$$\frac{d\ln m}{d\ln r} \cong \frac{\Delta\ln m}{\Delta\ln r} = \left(\ln\frac{\lambda_0(0)}{\lambda_0(\varepsilon_l)}\right)\bigg/\left(\ln\frac{r(\varepsilon_l)}{r(0)}\right).$$

The physical meaning of strain coefficients is that the process occurs at deformation of thin film in volume of the

grain (the increase of grain line size, the increase of lattice parameter, the deformation of lattice inner potential) and at the grain boundary (the deformation of grain boundary, turn of grains, relaxation processes related with the defects healing or defects generation, the initiation of localized energy levels).

In case of polycrystalline thin films it is necessary to use MS equation for the conductivity in multiplier for $A_1$ and $A_2$ in the equation (3.21). But this procedure is ineffective, besides, experimental and calculated data are unsatisfactory according to equation (3.21). The main reason is that the deformation depends on the parameter of specular reflection at the grain boundaries and the transmission parameter across the grain boundaries.

### 3.6.2 The macroscopic model

In the framework of macroscopic model for longitudinal strain we can ascertain that

$$\frac{d\ln\rho}{d\ln l} = \frac{d\ln\rho_1}{d\ln l} + \frac{d\ln\rho_2}{d\ln l} + \frac{d\ln(d_1+d_2)}{d\ln l} - \frac{d\ln(\rho_1 d_1 + \rho_2 d_2)}{d\ln l}.$$

This equation can be rewritten as

$$\gamma_l^\rho = \gamma_{l1}^\rho + \gamma_{l2}^\rho + \frac{\partial d_1/\partial\varepsilon_l + \partial d_2/\partial\varepsilon_l}{d_1 + d_2} -$$

$$- \frac{d_2\frac{\partial\rho_1}{\partial\varepsilon_l} + \rho_1\frac{\partial d_2}{\partial\varepsilon_l} + d_1\frac{\partial\rho_2}{\partial\varepsilon_l} + \rho_2\frac{\partial d_1}{\partial\varepsilon_l}}{\rho_1 d_2 + \rho_2 d_1}.$$

The index "$\rho$" signifies that $\gamma_l$ is defined through the resistivity $\rho$. If the derivatives are sequentially multiplied and divided by $d_1$, $d_2$, $\rho_1$, $d_2$, $\rho_2$ and $d_1$, then we receive

$$\gamma_l^\rho = \gamma_{l1}^\rho + \gamma_{l2}^\rho + \frac{d_1\mu_{f1} + d_2\mu_{f2}}{d_1 + d_2} -$$

$$-\frac{\gamma_{l1}^\rho\rho_1 d_2 - +\rho_1 d_2\mu_{f2} + \gamma_{l2}^\rho\rho_2 d_1 - \rho_2 d_1\mu_{f1}}{\rho_1 d_2 + \rho_2 d_1}. \qquad (3.22)$$

The analogical equation can be received for the coefficient of transverse strain.

The limiting forms of equation (3.22) are

$$\gamma_l^\rho \approx \gamma_{l1}^\rho + \gamma_{l2}^\rho - \mu_{f1} - \frac{\gamma_{l1}^\rho\rho_1 d_2 - \rho_2 d_1\mu_{f1}}{\rho_2 d_1} \approx$$

$$\approx \gamma_{l1}^\rho + \gamma_{l2}^\rho - \mu_{f1} - \gamma_{l2}^\rho + \mu_{f1} \approx \gamma_{l1}^\rho$$

$$at\ d_1 \to \infty,\ d_2 = const;$$

and

$$\gamma_l^\rho \approx \gamma_{l1}^\rho + \gamma_{l2}^\rho - \mu_{f2} - \frac{\gamma_{l1}^\rho\rho_1 d_2 - \rho_1 d_2\mu_{f2}}{\rho_1 d_2} \approx$$

$$\approx \gamma_{l1}^\rho + \gamma_{l2}^\rho - \mu_{f2} - \gamma_{l1}^\rho + \mu_{f2} \approx \gamma_{l2}^\rho$$

$$at\ d_1 = const,\ d_2 \to \infty.$$

The analysis of equation (3.22) in two limiting cases showed that size dependence of strain coefficient has the feature that value of strain coefficient for double-layered film system can increase ($\gamma_{g1}^\rho < \gamma_{g2}^\rho$) at decreasing thickness $d_2$ ($d_1 = const$) or decrease ($\gamma_{g1}^\rho > \gamma_{g2}^\rho$) working for to the asymptotic value $\gamma_{g2}^\rho$ (Fig. 3.5).

For multilayered film system with arbitrary number of layer and total thickness $d = d_1 + d_2 + \ldots + d_n$, the equation (3.22) can be rewritten as
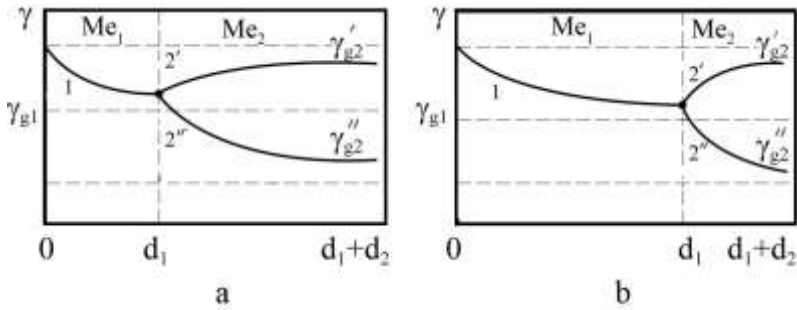
Figure 3.5 – The qualitative size dependences for double-layered films ($\gamma_1(d_1)$ (1), $\gamma_2(d_2)$ at $\gamma_{g2} > \beta_{g1}$ (2) and $\gamma_2(d_2)$ at $\gamma_{g2} < \beta_{g1}$) in two limiting cases: $d_1 = \text{const}$, $d_2 \to \infty$ (a), $d_2 = \text{const}$, $d_1 \to \infty$ (b)
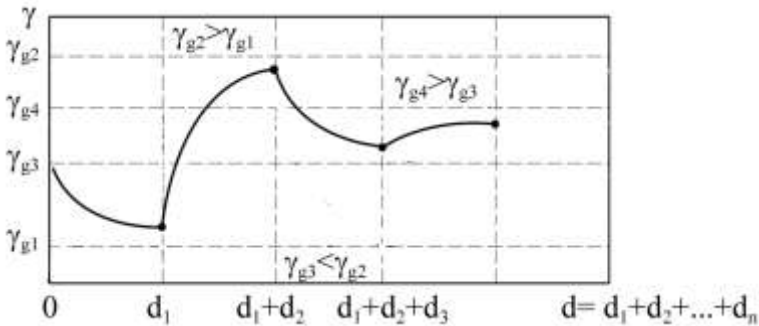


Figure 3.6 – The qualitative size dependences for multilayered film systems

$$\gamma_l^\rho = \sum_{i=1}^{n} \gamma_{li}^\rho - \frac{\sum_{i=1}^{n} d_i \mu_{fi}}{\sum_{i=1}^{n} d_i} - \frac{\sum_{i,k,m,...=1}^{n} d_i \left(\gamma_{lk}^\rho + \gamma_{lm}^\rho - \mu_{fi}\right) \rho_k \rho_m ...}{\sum_{i,k,m,...=1}^{n} d_i \rho_k \rho_m ...}.$$

(3.22')

Size dependence of strain coefficient of multilayered film system has nonmonotonic character: the value of strain coefficient will increase ($\gamma_{l1}^\rho < \gamma_{l2}^\rho < ... < \gamma_{ln}^\rho$), decrease (at reverse inequation) or oscillate working for corresponding asymptotic value $\gamma_g^\rho$ at increasing thickness $d_1$. In the frame of total multilayered system the value of strain coefficient will monotonously decrease (Fig. 3.6).

### 3.6.3 Interpretation of experiments

Values of $\gamma_l$ and $\gamma_t$ can be calculated by equations (3.17) and (3.18) using data for single-layered films. The results of comparison between experimental and calculated data for

Table 3.1 – Comparison between experimental and calculated data for strain coefficients of double-layered films

| Sample | Experimental data | | | | Calculated data | | |
|---|---|---|---|---|---|---|---|
| | $d_1$, nm | $d_2$, nm | $\beta \cdot 10^3$, $K^{-1}$ | $\gamma_l$ | $\eta_l$ | $\gamma_l$ | $S_T \cdot 10^{-8}$, Pa |
| Cr | 25–10 | | | | 2–4,3 | | |
| Ni | 20–120 | | | | 0,6–1,3 | | |
| Co | 20–65 | | | | 19,0 | | |
| Cr/Co | 90 | 60 | 2,60 | 26,7 | | 16,1 | 1,80 |
| Co/Cr | 60 | 65 | 2,25 | 21,0 | | 15,8 | 4,20 |
| Ni/Co | 30 | 80 | 3,38 | 13,5 | | 10,5 | 3,72 |
| Co/Ni | 50 | 55 | 3,40 | 9,0 | | 11,1 | 3,66 |

double-layered film systems based on Cr, Co and Ni are presented in Table 3.1. As we can see from Table 3.1 the deviation of one data from another is significant.

The reasons of deviations are as follows:

1) assumption that coefficients $p^*$ and $r$ do not depend on film strain;

2) interdiffusion of atoms from one layer to another;

3) presence of thermal expansion at interface between the layers.

### 3.7 Temperature dependence of strain coefficients

One of the least studied questions in the physics of thin films is the question about temperature dependence of strain coefficients.

On the basis of carried out analysis the conclusion on temperature dependence of strain coefficients can be made. In most general case we can write that $\gamma_l = C_1 + C_2 \cdot T$ and $\gamma_t = C_3 + C_4 \cdot T$. Thus, the value of longitudinal strain coefficient most probably will increase at temperature increase in case of
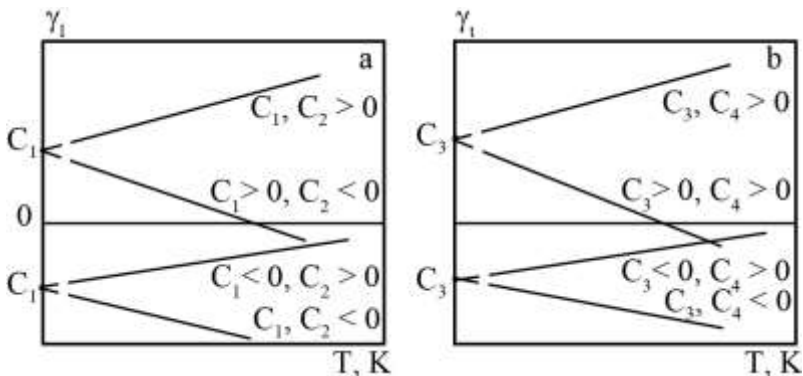


Figure 3.7 – Qualitative temperature dependence of longitudinal (a) transverse (b) strain coefficients

metal thin films and decrease at temperature increase in case of semiconductor films (Fig. 3.7).

On the assumption of more general considerations it is clear that strain coefficients must increase at temperature growth. According to our experimental data for Cr thin films temperature dependence of strain coefficients is linear and does not have peculiarities at points, which were described in previous subsections. The question about correlation temperature coefficients of strain $\beta_{\gamma l}$ and $\beta_{\gamma t}$ (TCS) and resistance was studied better. For obtaining the equation for these coefficients it is necessary to use the definition of TCS

$$\beta_{\gamma l} = \frac{1}{\gamma_l}\left(\frac{\partial \gamma_l}{\partial T}\right)_l, \ \beta_{\gamma t} = \frac{1}{\gamma_t}\left(\frac{\partial \gamma_t}{\partial T}\right)_t \qquad (3.23)$$

and equations (3.7) and (3.8). After differentiation with respect to temperature we obtain

$$\beta_{\gamma l} = \frac{1}{\gamma_l}\frac{\partial \gamma_l}{\partial T}\left(\frac{1}{\rho}\frac{\partial \rho}{\partial \varepsilon_l}+1+2\mu_f\right) = \frac{1}{\gamma_l}\left(-\frac{1}{\rho^2}\frac{\partial \rho}{\partial T}\frac{\partial \rho}{\partial \varepsilon_l}+\frac{1}{\rho}\frac{\partial^2 \rho}{\partial \varepsilon_l \partial T}\right),$$

$$\beta_{\gamma t} = \frac{1}{\gamma_l}\frac{\partial \gamma_l}{\partial T}\left(\frac{1}{\rho}\frac{\partial \rho}{\partial \varepsilon_t}-1\right) = \frac{1}{\gamma_l}\left(-\frac{1}{\rho^2}\frac{\partial \rho}{\partial T}\frac{\partial \rho}{\partial \varepsilon_t}+\frac{1}{\rho}\frac{\partial^2 \rho}{\partial \varepsilon_t \partial T}\right).$$

These equations can be rewritten in the form

$$\beta_{\gamma l} = \frac{1}{\gamma_l}\left(-\beta\frac{1}{\rho}\frac{\partial \rho}{\partial \varepsilon_l}+\frac{1}{\rho}\frac{\partial \rho}{\partial \varepsilon_l}\frac{\partial \varepsilon_l}{\partial \rho}\frac{\partial^2 \rho}{\partial \varepsilon_l \partial T}\right)$$

$$= \frac{\gamma_l - 1 - 2\mu_f}{\gamma_l}\left(-\beta\frac{1}{\gamma_l - 1 - 2\mu_f}\frac{1}{\rho}\frac{\partial^2 \rho}{\partial \varepsilon_l \partial T}\right), \qquad (3.24)$$

$$\beta_{\gamma_l} = \frac{1}{\gamma_t}\left(-\beta \frac{1}{\rho}\frac{\partial \rho}{\partial \varepsilon_t} + \frac{1}{\rho}\frac{\partial \rho}{\partial \varepsilon_t}\frac{\partial \varepsilon_t}{\partial \rho}\frac{\partial^2 \rho}{\partial \varepsilon_t \partial T}\right) =$$

$$= \frac{\gamma_t + 1}{\gamma_t}\left(-\beta \frac{1}{\gamma_t + 1}\frac{1}{\rho}\frac{\partial^2 \rho}{\partial \varepsilon_t \partial T}\right),$$

where $\dfrac{1}{\rho}\left(\dfrac{\partial \rho}{\partial \varepsilon}\right)_T$ is $\gamma_l - (2\mu_f + 1)$ and $\gamma_t + 1$ for longitudinal

and transverse strain coefficients, and $\dfrac{d\mu_f}{\partial T} = 0$ .

Subjected to $\gamma_l$ and $\gamma_t \geq 10$, equation (3.24) can be simplified to the form

$$\beta_{\gamma_l} \cong -\beta + \frac{1}{\rho \gamma_l}\cdot\frac{\partial^2 \rho}{\partial \varepsilon_l \partial T}, \quad \beta_{\gamma_t} \cong -\beta + \frac{1}{\rho \gamma_t}\cdot\frac{\partial^2 \rho}{\partial \varepsilon_t \partial T} \qquad (3.24')$$

which allows to determine the value of $\dfrac{\partial^2 \rho}{\partial \varepsilon_t \partial T}$ that characterizes the behaviour of strain sensor in the condition of temperature and deformation change. Note, that equations (3.24) and (3.24') are more precision in comparison with equation of Meiksin Z. $\beta_\gamma \approx -\beta$. The data for $\beta_\gamma$, $-\beta$ and $\dfrac{\partial^2 \rho}{\partial \varepsilon_t \partial T}$ are presented in Table 3.2.

Note that corresponding data for transverse strain are similar to data presented in Table 3.2.

Equations (3.24) and (3.24') allow to analyze the question for temperature dependence of $\gamma_l$ and $\gamma_t$.

In case of polycrystalline thin Me films, when $\beta > 0$ and $\dfrac{\partial^2 \rho}{\partial \varepsilon_t \partial T} > 0$, the value of $\beta_{\gamma_l}$ will be bigger than nought if

$$\frac{1}{\rho\gamma_l}\cdot\frac{\partial^2\rho}{\partial\varepsilon_l\partial T}>|\beta|,$$

that is realized according to Table 3.2 at $\rho\sim10^{-6}$–$10^{-7}$ Ohm·m.

In case of amorphous thin Me films or semiconductor thin films $\beta<0$ and value of $\beta_{\gamma_l}$ will be bigger than zero if

$$\frac{1}{\rho\gamma_l}\cdot\frac{\partial^2\rho}{\partial\varepsilon_l\partial T}>|\beta|\text{ and }\frac{\partial^2\rho}{\partial\varepsilon_l\partial T}>0.$$

At the same time $\beta_{\gamma_l}<0$ if $\dfrac{\partial^2\rho}{\partial\varepsilon_l\partial T}<0$ at $\beta>0$.

In case when $\dfrac{\partial^2\rho}{\partial\varepsilon_l\partial T}<0$, $\beta_{\gamma_l}<0$ if $\left|\dfrac{1}{\rho\gamma_l}\cdot\dfrac{\partial^2\rho}{\partial\varepsilon_l\partial T}\right|>|\beta|$.

In opposite case, when $\left|\dfrac{1}{\rho\gamma_l}\cdot\dfrac{\partial^2\rho}{\partial\varepsilon_l\partial T}\right|<|\beta|$, parameter $\beta_{\gamma_l}$ will have positive value.

Table 3.2 – Parameter of strain sensibility for polycrystalline and amorphous thin films ($T=300$ K)

| Film | $\beta\cdot10^{-3}$, $K^{-1}$ | $\gamma_l$ | $\beta_{\gamma_l}\cdot10^{-3}$, $K^{-1}$ | $\dfrac{\partial^2\rho}{\partial\varepsilon_t\partial T}, \dfrac{Ohm\cdot m}{K}$ |
|---|---|---|---|---|
| Cr (poly) | 0,70 | 2,0 | 6,0 | $4,5\cdot10^{-9}$ |
| Mo (poly) | –0,09 | 13,5 | 9,9 | $11,4\cdot10^{-9}$ |
| Mo(amorph.) | –0,20 | 36,6 | 10,6 | $38,0\cdot10^{-8}$ |

In conclusion of strain effect discussion it is necessary to emphasize that strain properties have been investigated for Au, Pd, Pt, Co, Ni, Al, Sb, Te, Cr, Mo, W etc. thin films and thin film systems based on them. It is obvious, that such thin

film materials can be used as strain sensor if they have stable and resettability parameters. The artificial ageing of thin films at the heat treatment a little improved stability of strain parameters but did not meet the real problem. Stability of strain properties of thin film materials increases if deposit of thin silicon oxide layer is applied on the top of thin film or deposit of thin film on the $Al_2O_3$ layer were previously applied on substrate by method of RF sputtering. Although it does not solve the problem of thermal stability of strain parameters.

### 3.8 Problems

#### Problem # 1
On the basis of the definition of strain coefficients $\gamma_l$ and $\gamma_t$, show that $\gamma_l = \dfrac{d\rho}{\rho_n d\varepsilon_\ell} + \left(1 + 2\mu_f\right)$ and $\gamma_t = \dfrac{d\rho}{\rho_n d\varepsilon_t} - 1$.
Show that summands $\dfrac{d\rho}{\rho_n d\varepsilon_\ell}$ and $\dfrac{d\rho}{\rho_n d\varepsilon_t}$ can be substituted by

$-\dfrac{d\sigma}{\sigma_n d\varepsilon_\ell}$ and $-\dfrac{d\sigma}{\sigma_n d\varepsilon_t}$ respectively.

#### Problem # 2
Prove that for bulk materials the equation for the longitudinal strain coefficient can be written as $\gamma_l \cong \eta_l + 2(1 + \mu)$.

*Directive*: it is necessary to use the equation for conductivity $\sigma \cong n\lambda_0$, where $n$ is the electron concentration, and theoretical evaluation $-\left(\dfrac{dn}{n \cdot d\varepsilon}\right) \cong 1$.

**Problem # 3**

On the base of the definition of temperature coefficients of strain $\beta_{\gamma_l}$ and $\beta_{\gamma_t}$, prove that in the limiting case of large values of $\gamma_l$ and $\gamma_t$:

$$\beta_{\gamma_\ell} \cong -\beta + \frac{1}{\rho_n \cdot \gamma_{\ell n}} \cdot \frac{\partial^2 \rho}{\partial T \partial \varepsilon_l}$$

and

$$\beta_{\gamma_t} \cong -\beta + \frac{1}{\rho_n \cdot \gamma_{tn}} \cdot \frac{\partial^2 \rho}{\partial T \partial \varepsilon_t} \,.$$

In what case $\beta_\gamma \cong -\beta$ ?

**Problem # 4**

Show qualitatively size dependences of $\gamma_l$ and $\gamma_t$ (in width range of thickness) in the frame of the Fuchs and Sondheimer model.

**Problem # 5**

Why the Fuchs and Sondheimer model in strain is not agreed with experimental data?

### 3.10 References

1. Бурик І. П. Тензорезистивні властивості плівкових матеріалів на основі Mo, Ni та Fe / І. П. Бурик, Т. М. Гричановська, Л. В. Однодворець // Металлофиз. новейшие технол. – 2010. – Т. 32, No. 3. – С. 345–356.
2. Забіла Є. О. Методика вивчення тензорезистивних властивостей плівок хрому при відносно малих і великих деформаціях / Є. О. Забіла, І. Ю. Проценко // УФЖ. – 2005. – Т. 50, No. 7. – С. 729–736.

3. Однодворець Л. В. Електрофізичні та магніторезистивні властивості плівкових матеріалів в умовах фазоутворення / Л. В. Однодворець, С. І. Проценко, А. М. Чорноус. – Суми : Сумський державний університет, 2011. – 204 с.

4. Пазуха І. М. Фізичні властивості плівкових матеріалів мікро- і наноелектроніки : навчальний посібник / І. М. Пазуха, І. Ю. Проценко, І. В. Чешко ; за заг. ред. І. Ю. Проценка. – Суми : Сумський державний університет, 2014. – Ч. 2. – 212 с.

5. Проценко І. Ю. Тонкі металеві плівки (технологія та властивості) : навчальний посібник / І. Ю. Проценко, В. А. Саєнко. – Суми : Сумський державний університет, 2002. – 187 с.

6. Проценко С. І. Структурно-фазовий стан, стабільність інтерфейсів та електрофізичні властивості двошарових плівкових систем (огляд) / С. І. Проценко, Л. В. Однодворець, А. М. Чорноус, І. Ю. Проценко // Успехи физ. мет. – 2007. – Т. 8, No. 2. – С. 109–156.

7. Дехтярук Л. В. Эффект тензочувствительности в поликристаллических многослойных структурах общего типа / Л. В. Дехтярук, С. И. Проценко, А. Н. Чорноус // Тонкие пленки в оптике и электронике. – Харьков : ННЦ ХФТИ. – 2003. – С. 185–188.

8. Кузьменко А. И. Эффект тензочувствительности в двухслойных пленках переходных металлов / А. И. Кузьменко, С. В. Петренко, И. Е. Проценко // ВАНТ. Серия : Ядерно-физические исследования. – 1990. – Вып. 2. – С. 87–89.

9. Мейксин З. Г. Физика тонких пленок / З. Г. Мейксин . – Москва: Мир, 1978. – Т. 7. – С. 106–179.

10. Buryk I. P. Tensoresistive effect in thin metal films of the range of elastic and plastic strain / I. P. Buryk,

D. V. Velykodnyi, L. V. Odnodvorets et. al // Tech. Phys. – 2011. – Vol. 56, No. 2. – P. 232–237.

11. El-Hiti M. Dependence of temperature coefficient of the strain coefficients of resistance of double-layer thin metallic films of thermal strains / M. El-Hiti // Phys. Stat. Sol. (A). – 1989. – Vol. 155, No. 1. – P. 185–189.

12. Khater F. Strain coefficients of electrical resistance of double-layer thin metallic films / F. Khater, M. El-Hiti // Phys. Stat. Sol. (A). – 1988. – Vol. 108, No. 1. – P. 241–249.

13. Khater F. Temperature coefficient of the strain coefficient of electrical resistivity of double-layer thin metallic films / F. Khater, M. El-Hiti // Phys. Stat. Sol. (A). – 1988. – Vol. 109, No. 2. – P. 517–523.

14. Lasyuchenko O. Microscopic theory of tensosensibility of multilayer polycrystalline films / O. Lasyuchenko, L. Odnodvoretz, I. Protsenko // Cryst. Res. Technol. – 2000. – Vol. 35, No. 3. – P. 329–332.

15. Ma D. Evaluation of the mechanical properties of thin metal films / D. Ma, K. Xu, J. He, J. Lu // Surf. Coating Tech. – 1999. – Vol. 116–119. – P. 128–132.

16. Protsenko I. Yu. Electroconductivity and tensosensibility of multilayer films / I. Yu. Protsenko, L. V. Odnodvorets, A. M. Chornous // Metallofiz. Noveiishie Technol. – 1998. – Vol. 20, No. 1. – P. 36–44.

17. Protsenko I. Yu. Strain properties of granular film alloys / I. Yu. Protsenko, L. V. Odnodvorets, K. V. Tyschenko, M. O. Shumakova // J. Mech. Eng. Technol. – 2013. – Vol. 1, No. 1. – P. 34–39.

18. Protsenko S. I. Future strain properties of multilayer film materials. Book Nanocomposites, Nanophotonics, Nanobiotechnology and Applications / S. I. Protsenko, L. V. Odnodvorets, I. Yu. Protsenko; edited by O. Fesenko, L. Yatsenko. – Cham – Heidelberg – New York – Dordrecht

– London : Springer International Publishing Switzerland, 2015. – Ch. 28. – P. 345–374.

19. Tellier C. R. Size effects in thin films / C. R. Tellier, A. J. Tosser. – New York : Elsevier, 1982. – 310 p.

20. Tyschenko K. V. Electrophysical properties on nanocrystalline platinum thin films / K. V. Tyschenko, I. M. Pazukha, T. M. Shabelnyk, I. Yu. Protsenko // J. Nano-Electron. Phys. – 2013. – Vol. 5, No. 1. – P. 01029–1–01029–5.

# Conclusion

The range of thin film materials application is so wide and numerous, that we can talk about new technological direction – thin film matter science. It is, first of all, wide application in submineering of electronics, post and disc support for coaxial systems, plate hearing for wave systems, bolometers and thermoelements, strain sensor with high sensibility, application of magnetic thin films as logic or magnetic components, instrument engineering technical direction of applied character in thin films. Thin films with thickness in the range from ten nanometers to several microns are used at thin film elements production. Common preparation of many elements like resistors, capacitors, inductance, contacts etc. exclude the stage of elements arrangement and allows reducing their cost price. The modern stage of microelectronic development is characterized by using integrated circuits (IC). Their development and innovation allow developing big integrated circuits (BIC) with high scale of integration and complication of functions. On the base of BIC chip the computer has been developing. The main element of computer becomes microprocessor.

The first microprocessor (was developed in 70th of 20th century) took several plated circuit. Very large scale integrated circuits appeared subsequently and microelectronic circuits received application in other technical devices.

Describe the ways of introducing metal films in microelectronics in brief.

## C1. Resistors on the base of thin films

For the first time patent on the using Me thin film as resistor was received by the Englishmen F. Kruger in 1919. Thereafter thin film resistors were widely used and

successfully compete with bulk resistors, which have size less then 130 μm (precision resistors with sizes 130–260 μm are economically sound in comparison with thin film resistors only). Thin film resistors can be prepared both as discrete type and as a part of integrated circuits.

Thin Me films which have sheet resistance $R = 10$–1000 Ohm are more particularly used at resistors preparation. Note, that $R$ is resistance of sample with length $l$ which is equal to width a, so $R = \rho/d$. Besides corresponding value of $R$, thin films must have small value of temperature coefficient of resistance (less than $10^{-4}$ $K^{-1}$) and good stability of parameters. Any change of resistance during the work of resistor should not transcend permissible value. In the end, technology of resistors preparing should ensure their low cost.

Summarizing results of Section 3, it is necessary to note such reasons of Me thin films high resistance:

– size effects of Fuchs – Sondheimer and Mayadas – Shatzkes in electrical conductance and TCR, although these effects are seldom used at the resistors preparing;
– thin film may have much larger quantity of impurities and crystalline defects in comparison with equilibrium because of low value of TCR and high value of resistance. For comparison, note, that dislocations, vacancies, penetration atoms, grain boundaries and equilibrium impurities give additional resistance: $0{,}1 \cdot 10^{-8}$; $0{,}5 \cdot 10^{-8}$; $1 \cdot 10^{-8}$; $40 \cdot 10^{-8}$ and $180 \cdot 10^{-8}$ Ohm·m respectively;
– two-phase thin film (cermet or of the type "metal-insulator"), in which conducting phase is dissolved in insulator solution;
– thin films with small density (porous films) have high resistance and low TCR but they have large surface area and need protection from high-speed oxidation;
– multilayered thin films in which separate layers have different TCR in sign; resistors with high resistance and low TCR were received as a result of such combination;

– new crystal structures with low concentration of charge carrier (well-known example of such structure is $\beta$-Ta).

Different types of alloys, metal systems like cermets and semiconductors are used for resistors production.

Nichrome (80 % Ni + 20 % Cr) is one of the best alloy for resistor preparing. The value of resistance of thin nichrome films changes in the range from 5 to 400 Ohm/□ and temperature coefficient of resistance changes in the range from $-100 \cdot 10^{-6}$ to $200 \cdot 10^{-6}$ K$^{-1}$. An effort of receiving thin films with higher value of resistivity in comparison with nichrome was done. With this purpose Ni atoms were exchanged into Si atoms. As a result the value of TCR takes $\pm 5 \cdot 10^{-4}$ K$^{-1}$.

In connection with the problem of composition control of the alloy the monometallic resistors are more perspective. Currently, the Ta thin films are widely used at resistors preparing because these electrical properties are better in comparison with another heat-resisting material (Ti, Hf, Mo, W, Re, Ct et al.). The electro-physical properties of tantalum thin films subject to preparation condition are presented in Figure C1.
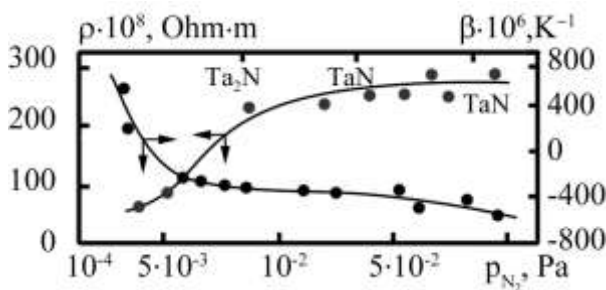


Figure C1 – Nitrogen influence on resistivity and TCR of tantalum thin films

The most successful result among bundle of compositions of metal-insulators that were investigated in the state of thin film was obtained in the system of Cr-SiO. The value of resistivity and TCR of Cr-SiO corresponding to SiO concentration changes in the range $(80–6000) \cdot 10^{-8}$ Ohm·m and $(−800–100) \cdot 10^{-6}$ K$^{-1}$. The other cermets (Cr-MgF, Au-SiO, Pt-TaO, Au-WO, Au-TaO) were also investigated, but they did not prove the resistance range and stability like a Cr-SiO system.

## C2. Thin film capacitors

The technology of thin film IC provides formation of bundle resistors, capacitors and junctions on the insulator substrate. Thin films with chemical and temperature stabilities are used at capacitor preparing. Insulator thin films like TaO (dielectric constant $\varepsilon = 25$), Al$_2$O$_3$ ($\varepsilon = 25$), SiO ($\varepsilon = 6$), SiO$_2$ ($\varepsilon = 4$) are most widely used at capacitor preparing. The schematic structure of tantalum capacitor (basic type) is presented in Figure C2.
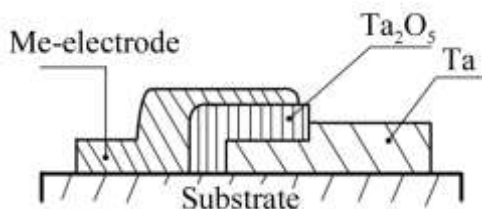


Figure C2 – The basic type of the tantalum capacitor

Insulators like Mn$_2$O$_3$, MnO$_2$, SiO can be used in return for TaO in another type of capacitors. As a metal electrode (top armature) thin films likes Au, Pd, Sb, Gd, Fe, In, Al, etc. can be used. At their combination with insulator substrate Ta$_2$O$_5$ the intensity of electric field breakdown $E = U_b/d$, where $U_b$ is

the voltage of capacitor breakdown, $d$ is insulator thickness, and takes value $(0,64–4,12) \cdot 10^8$ V/m at requirement $10^7$–$10^9$ V/m.

Very important characteristic of capacitor is stability at voltage, temperature and humidity test. The special investigations were carried out for determination of these characteristics.

## C3. Superconductor thin films and devices based on them

D. Bak in 1956 proposed the device cryotron, which can be used as computing element. It consists of tantalum superconducting element (gate) enclosed by solenoid from niobium wire. Tantalum conductor can be taken out from superconductor state by magnetic field which is generated by niobium solenoid. The analysis showed that gate can be prepared as thin film and in 1959 V. Newhouse and J. Bremer constructed thin film cryotron. This cryotron consisted of solenoid of tin thin film isolated from gate layer by SiO interlayer.

If valve of cryotron contains in the middle point of transition from superconductor to normal state, then negligible increase of current control may set conditions for significant change of current or voltage through the valve. Such highly complex system allows intensifying current that flows through gate.

Cryotron may be of the wire-wound or crossed-film (flat) type. The design of crossed-film cryotron is presented in Figure C4.

Some properties of cryotron allow using it as switching or storage and logic device.

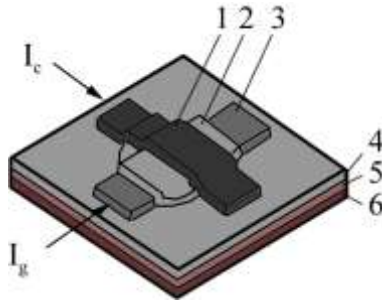Quite a number of application examples of superconductor thin films at developing different devices can

Figure C3 – The design of crossed-film cryotron:
1 – control film (Pd); 2 – insulating layer ($SiO_2$); 3 – gate film
(Sn); 4 – insulating layer ($SiO_2$); 5 – ground plane; 6 – substrate.
$I_c$ – control electric current; $\underline{I}_g$ – gate electric current

be done. One of them is bolometer. Bolometer on the basis of
the tin thin film has sensibility $10^{-12}$ Watt. Storage cell of
Josephson is widely used.

## C4. Thin film sensors

Sensors in the broadest sense of the word are master
nodes of electronic circuit for measuring nonelectric
parameters located directly near the object.

The technology of sensors design and application was
developed in independent direction of measurement
technology. Since main requirements to sensor are minimal:
low cost, mechanical strength, so the technology of their
preparing is the same as for preparing semiconductor integrated
circuits (thin-film and thick-film technologies of sensors
preparing are compatible with microelectronic technology).

Pt and Ni thin films are used as temperature sensors. The
design of thin film thermoresistor is presented in Figure C4.

Principle of operation of strain sensor is based on strain
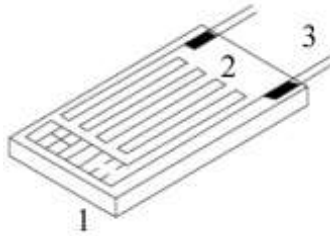measurement of resistance strain gauge which is formed into Si

95

Figure C4 − The design of thin film thermoresistor:
1 − substrate; 2 − thin film sensitive element (mono- of multilayered thin film system); 3 − leads
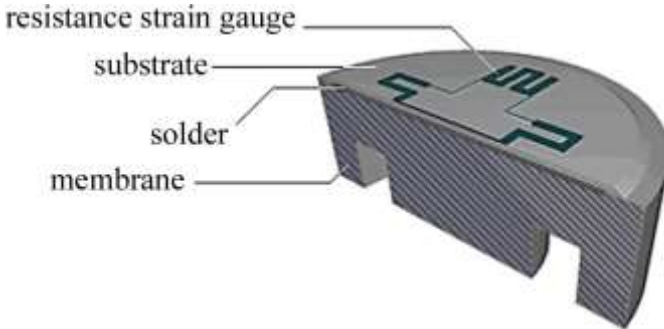


Figure C5 − The design of converter on the base of thin film resistance strain gauge

epitaxial thin film on the top of sapphire substrate soldered by brazen alloy to titanium membrane (Figure C5).

Pressure sensors (barometer) are prepared from Si template with etched membrane. Strain elements deposit on the top of membrane by method of implantation or deposition.

Humidity measurement can be done using dry and wet bulb hygrometers, dew point hygrometers, and electronic hygrometers. There is a surge in the demand of electronic hygrometers, often called humidity sensors. Humidity sensors

determine the amount of water vapour present in a gas that can be a mixture, such as air, or a pure gas, such as nitrogen or argon.

Humidity sensors can be broadly divided into two categories: one employs capacitive sensing principle, while other uses resistive effects (Figure C6).

In case of capacitive type humidity sensor (Figure C6, a), lower electrode is formed using gold, platinum or other material on alumina substrate. A polymer layer such as PVA is deposited on the electrode. This layer senses humidity. On the top of this polymer film, gold layer is deposited which acts as top electrode. The upper electrode also allows water vapour to pass through it into the sensing layer. The vapour enters or leave the hygroscopic sensing layer until the vapour content is in equilibrium with the ambient air or gas. Thus, capacitive type sensor is basically a capacitor with humidity sensitive polymer film as the dielectric.

In case of resistive type humidity sensors (Figure C6, b) thick film conductor of precious metals like gold, ruthenium oxide is printed and calculated in the shape of the comb to form an electrode. Then a polymeric film is applied on the electrode; the film acts as a humidity sensing film due to the existence of movable ions. Change in impedance occurs due to change in the in the number of movable ions.
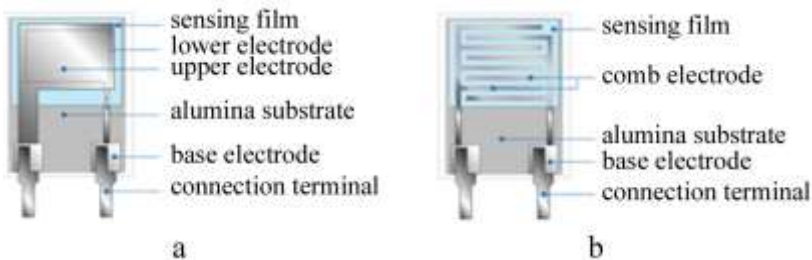


Figure C6 – Basic structures of capacitive type (a) and resistive type (b) humidity sensors

Thin film system Ti/Si is used as a sensor of ammonia. On the base of monophase thin films $TiO_{0,2}$, $TiO_{0,5}$, $TiO_{0,7}$–$TiO_{1,3}$, $TiO_{1,4}$ layered structures Me/oxide/semiconductor and Me/oxide/Me were realized.

Thin film system $Au/SnO_2/Au$ is used as humidity sensor on the base of capacity measurement with dry or moist insulator $SnO_2$. Thin films $SnO_2$ become sensitive to humidity after annealing at oxygen atmosphere or without annealing by method of low-temperature formation of gas sensitive layer.

The principle of nitric oxide sensor operation is based on changes of transmission coefficient as a result of thin film systems $A^I Bi(Ge)C^{VI}$ oxidation, where $A^I$ is Li, K, Rb; $C^{VI}$ is S, Se.

Thin film system $Pt/LaF_3/SiO_2/SiC$ is successfully used for chlorofluorocarbon (Freon) registration.

It is known that low-dimensional organic materials found a successful application in the strain sensor technology, as such materials have value of strain coefficient – 100–1000. Essential fault of such films is very low thermal stability like a semiconductor strain sensors.

In this connection multilayered film systems on the base of Cr, Ni and other metal are more effective than sensing elements of high-temperature strain sensors. The value of strain coefficient of such multilayered systems is equal to 10. Such strain sensors have practical application as mechanical motion transducer.

## C5. References

1. Проценко І. Ю. Датчики неелектричних величин : навчальний посібник / І. Ю. Проценко, Н. І. Шумакова. – Суми : Сумський державний університет, 2003. – 79 с.
2. Проценко І. Ю. Тонкі металеві плівки (технологія та властивості) : навчальний посібник / І. Ю. Проценко, В. А. Саєнко. – Суми : Сумський державний університет, 2002. – 187 с.
3. Швець Є. Я. Матеріали і компоненти електроніки : навчальний посібник / Є. Я. Швець, І. Ф. Червоний, Ю. В. Головко. – Запоріжжя : ЗДІА, 2011. – 278 с.
4. Блех А. Тонкие пленки в интегральных схемах // Технология тонких пленок / под ред. Л. Майссела, Р. Глэнга. – Москва : Сов. радио. – 1977. – Т. 2. – С. 724–753.
5. Герштенберг Д. Тонкопленочные конденсаторы // Технология тонких пленок / под ред. Л. Майссела, Р. Глэнга. – Москва : Сов. радио. – 1977. – Т. 2. – С. 623–665.
6. Джойсон Р. Э. Тонкие сверхпроводящие пленки и устройства на их основе // Технология тонких пленок / под ред. Л. Майссела, Р. Глэнга. – Москва : Сов. радио. – 1977. – Т. 2. – С. 666–722.
7. Майссел Л. И. Тонкопленочные резисторы // Технология тонких пленок / под ред. Л. Майссела, Р. Глэнга. – Москва : Сов. радио. – 1977. – Т. 2. – С. 623–665.
8. Пленочные термоэлементы : физика и применение / под ред. Н. С. Лидоренко. – Москва : Наука, 1985. – 232 с.
9. Anwarzai B. Pseudo spin-valve on plastic substrate as sensing elements of mechanical strain / B. Anwarzai, V. Ac, S. Luby // Vacuum. – 2010. – Vol. 84. – P. 108–110.
10. Chung G.-S. Characteristics of tantalum nitride thin film strain gauges for harsh environments / G.-S. Chung // Sens. Actuat. A. – 2007. – Vol. 135. – P. 355–359.

11. Heckmann U. New materials for sputtered strain gauges / U. Heckmann, R. Bandorf, H. Gerdes et al. // Procedia Chemistry. – 2009. – Vol. 1. – P. 64–67.

12. Hrovat M. A characterisation of thick film resistors for strain gauge applications / M. Hrovat, D. Belavic, Z. Samardzija, J. Holc // J. Mater. Sci. – 2001. – Vol. 36. – P. 2679 – 2689.

13. Lichtenwalner D. J. Flexible thin film temperature and strain sensor array utilizing a novel sensing concept / D. J. Lichtenwalner, A. E. Hydrick, A. I. Kingon // Sens. Actuat. A. – 2007. – Vol. 135. – P. 593–597.

14. Mitin V. F. Resistance thermometers based on the germanium films / V. F. Mitin // Quantum Electronics and Optoelectronics. – 1999. – Vol. 2, No 1. – P. 115–123.

15. Electrical properties of nickel oxide thin films for flow sensor application / S. Noh, E. Lee, J. Seo et al. // Sens. Actuat. A. – 2006. – Vol. 125. – P. 363–366.

16. Schmid-Engel H. Strain sensitive Pt-SiO$_2$ nano-cermet thin films for high temperature pressure and force sensors / H. Schmid-Engel, S. Uhlig, U. Werner // Sens. Actuat. A : Phys. – 2014. – Vol. 206. – P. 17– 21.

17. Strain sensitivity of TiB$_2$, TiSi$_2$, TaSi$_2$ and WSi$_2$ thin films as possible candidates for high temperature strain gauges / G. Schultes, M. Schmitt, D. Goettel et al. // Sens. Actuat. A. – 2006. – Vol. 126. – P. 287–291.

18. Sensor and microelectronic elements based on nanoscale granular systems (review) / S. A. Nepijko, D. Kutnyakhov, L. V. Odnodvorets et al. // J. Nanopart. Res. – 2011. – Vol. 12 (13). – P. 6263–6281.

19. Suhao H. Thin film temperature sensor for real-time measurement of electrolyte temperature in a polymer electrolyte fuel cell / H. Suhao, M. M. Matthew, T. Srinivas // Sens. Actuat. A. – 2006. – Vol. 125. – P. 170–177.

20. Sung-Pil Chang. Demonstration for integrating capacitive pressure sensors with read-out circuitry on stainless steel substrate / Sung-Pil Chang, Mark G. Allen // Sens. Actuat. A. – 2004. – Vol. 116. – P. 195–204.
21. Yeung K. W. Micro-pressure sensors made of indium tin oxide thin films / K. W. Yeung, C. W. Ong // Sens. Actuat. A. – 2007. – Vol. 137. – P. 1–5.